Mechanical properties of 3D-printed temporary crown resin materials in accordance to different acidity

Myoung-Ji Choi

Department of Dentistry

The Graduate School, Yonsei University

Mechanical properties of 3D-printed temporary crown resin materials in accordance to different acidity

Directed by Professor Jae-Sung Kwon

The Doctoral Dissertation
submitted to the Department of Dentistry,
the Graduate School of Yonsei University
in partial fulfillment of the requirements
for the degree of Ph.D. in Dental Science

Myoung-Ji Choi

February 2024

This certifies that the Doctoral Dissertation of ‘Myoung-Ji Choi’ is approved.

Thesis Supervisor: Jae-Sung Kwon

Thesis Committee Member#1: Kwang-Mahn Kim

Thesis Committee Member#2: Kyung Chul Oh

Thesis Committee Member#3: Sang-Bae Lee

Thesis Committee Member#4: Eun-Jung Lee

The Graduate School
Yonsei University

February 2024

ACKNOWLEDGEMENT

학업에 대한 열망과 갈증으로 시작하게 된 대학원 생활은 직장 일과 함께 병행하는 것이 쉽지만은 않았습니다.
제 인생에 새로운 도전이였고, 새로운 꿈을 꾸게 만들어준 4년 반의 박사과정은 제게 선물과도 같았습니다.
감사의 말씀을 전하기엔 턱없이 부족하지만 지난 시간동안 제 곁에서 저를 위해 도움을 주신 모든 분들께 이 지면을 이용해 감사의 인사를 드립니다.
부족하지만 이 논문이 완성될 수 있도록 지도와 격려로 이 자리까지 이끌어 주신 권재성 지도교수님께 깊은 감사의 인사를 드립니다. 더하여 바쁘신 와중에도 논문에 관심을 가지고 지도해 주시며, 때로는 따뜻하게 때로는 날카롭게 지적해 주셨던 김광만 교수님, 오경철 교수님, 이상배 박사님, 이은정 교수님께 감사의 인사를 전합니다. 연구자로서 부족한 점이 많았던 저를 위해 많은 가르침과 길을 알려주신 덕분에 무사히 논문을 작성하고 박사 학위를 마칠 수 있었습니다.
또한 저에게 큰 도움을 준 교정과 유재훈 선배님, 재료학 교실 정일준 선배님, 졸업 동기 최지원 선생님, 강릉원주대 보철과 송민규 선생님께도 감사의 마음을 함께 전하고 싶습니다.

마지막으로 격려와 함께 도움을 주신 가족들에게도 깊은 사랑과 감사 인사를 전하고 싶습니다. 여러 어려움을 함께 극복하며 물심양면 지지해 주신 부모님, 항상 멀리서도 응원과 격려를 해준 친 오빠 최성진, 논문이 완성되면 함께 크게 기뻐해줄 친구 서승아, 이무혁에게도 감사의 마음을 전하고 싶습니다.
다시 한번, 모든 분께 깊은 감사의 인사를 전하며 학문의 여정에서 배움에 깊이를 더한 만큼 앞으로 배워야 할 것이 더 많음을 깨닫고, 겸손한 마음으로 나아가도록 하겠습니다.
감사합니다.

2024년 1월 저자 씀

TABLE OF CONTENTS

LIST OF FIGURES

LIST OF TABLE

ABSTRACT

Mechanical properties of 3D-printed temporary crown resin materials in accordance to different acidity

Myoung-Ji Choi

Department of Dentistry

The Graduate School, Yonsei University

(Directed by Professor Jae-Sung Kwon, M.D., Ph.D.)

Recently, the digital industry has established itself as a major technology in the field of dentistry. Additive manufacturing (AM)

technology has rapidly emerged as a key technology for digital dentistry. Temporary dental restorations are also produced using various additive manufacturing technologies. Additionally, dietary habits expose these temporary restorations to factors such as sugary food and acidic drinks.

Thus, the objective of this study was to investigate the influence on the mechanical properties of temporary restorations produced from AM technology when exposed to different acidic pH levels, as well as the mechanical properties of fabricated temporary resin specimens through different AM technologies.

A total of 180 rectangular parallelepiped-shaped specimens, 60 bar-shaped specimens, and 15 disk-shaped specimens were prepared using three different types of printing methods to produce dental resin crowns: Stereolithography Apparatus (SLA), Digital Light Processing (DLP), and Fused Deposition Modeling (FDM). All specimens were stored in two different pH levels of 4 and 6 and aged for one month in conditions simulating those of the oral environment at 37 ℃.

The water absorption and solubility measurements were performed to confirm the physical properties. The Knoop surface hardness, flexural strength, and wear resistance measurements were performed to confirm the mechanical properties. The water absorption, solubility, and flexural strength were evaluated according to ISO 4049 to verify that the three

different types of printing methods used for the dental resin crown meet the calibration requirements. To measure Knoop surface hardness, each specimen was tested under a 500gf load and 15 seconds dwell time, with three repeated measurements. To measure the wear resistance of the three different types of printing specimens, zirconia and cobalt-chrome alloy antagonists were used. Each specimen was then subjected to 20,000 cycles of chewing simulations with a 5 mm vertical descending movement and 2 mm horizontal movement under a 5 kg load. One-way ANOVA, Tukey's post-hoc analysis, Mann-Whitney, and T-test were used for comparison.

The SLA and DLP groups showed no significant difference in Knoop surface hardness, flexural strength, and wear resistance ($p > 0.05$). However, the FDM group significantly decreased Knoop surface hardness, flexural strength, and wear resistance compared to the other two groups ($p < 0.05$).

For the Knoop surface hardness test and flexural strength test, all specimens showed a significant decrease in surface hardness and flexural strength values ($p < 0.05$) in the presence of pH 4.0, regardless of the methods used to produce them. For the wear resistance test, all specimens showed a significant increase in wear volume loss and maximal depth loss values ($p < 0.05$) in the presence of pH 4.0, regardless of the methods used to produce them.

In conclusion, despite the limitations of this *in vitro* experiment, the SLA and DLP groups showed greater mechanical properties compared to the FDM group. The acidic pH environment resulted in more destructive and weaker mechanical properties in all groups. When temporary restorations are clinically used, it is important to determine the method of additive manufacturing and pay attention to acidity.

Key words; AM technologies, SLA, DLP, FDM, temporary restoration, acidic pH, mechanical properties

Mechanical properties of 3D-printed temporary crown resin materials in accordance to different acidity

Myoung-Ji Choi

Department of Dentistry
The Graduate School, Yonsei University

(Directed by Professor Jae-Sung Kwon, M.D., Ph.D.)

I. INTRODUCTION

1. Additive manufacturing (AM) technology

Recently, the digital industry has established itself as a major technology in the field of dentistry. In particular, additive manufacturing (AM) technology has been rapidly emerging as a key technology for

digital dentistry (Lee 2016). It has been utilized in a wide range of clinical applications including prosthodontics, maxillofacial surgery, orthodontics, oral implantology, and other fields, and it also has great potential advantages (Tian et al. 2021).

AM technologies used in dentistry include stereolithography (SLA), digital light processing (DLP), fused deposition modeling (FDM), selective laser sintering (SLS), etc (Tian et al. 2021).

SLA and DLP technology are among the most representative additive manufacturing processes for dentistry. These technologies, based on photopolymers, are used in VAT polymerization (Schweiger 2021). The advantages of this technology include excellent detail resolution (Javaid 2019, Unkovskiy 2018), high mechanical strength and good surface quality (Daule 2013). FDM technology has been rapidly emerging as a popular technology due to its environmentally filamentous thermoplastic material, which is suitable for use in the oral cavity (Tian et al. 2021).

To utilize AM technology for clinical purposes, the individual characteristics of the printed outcome must be understood.

2. AM technology type

2.1. SLA technology

SLA is a representative additive manufacturing technology known as vat photopolymerization (Ligon et al. 2017).

The machine consists of a vat that contains liquid polymer resin, a printing bed, a building platform upon which the object is built, a light source, and scanning mirrors for guiding the laser beam (Mukhtarkhanov 2020) (**Figure 1**).

The working principle of SLA is to expose the movable light source to activate photopolymerization (Hull 1984) and build up the photocurable liquid resin in a point-by-point method for the construction of objects. The strategy behind the vat photopolymerization (also known as photo-cross-linking) is based on using monomers in a liquid state and photo initiator molecules (like acrylates) as UV reacts with monomers and binds them together (Pandey 2014). This photo-cross-linking process induces an improvement in the chemical resistance and mechanical properties of the polymer (Pandey 2014).

This advantages of the SLA technology include excellent detail resolution (Javaid 2019, Unkovskiy 2018), high mechanical strength and good surface quality (Daule 2013).

However, it takes a long time to print, and the equipment and materials

involved in SLA are expensive. Additionally, it is difficult for beginners to clean due to the sticky and messy photopolymer used.

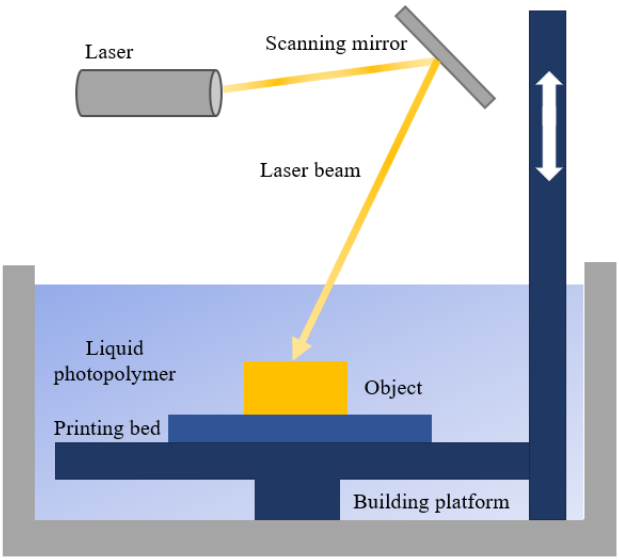

Figure 1. Schematic diagram of stereolithography technology.

2.2. DLP technology

DLP is one of the most popular additive manufacturing processes for dentistry.

The design of DLP technology is similar to SLA , with the main difference being the light source used (Schweiger 2021) (**Figure 2**). DLP technology features the use of a light source that illuminates each layer all at once, as opposed to SLA which uses point-by-point exposure (Soman et al. 2013). Therefore, DLP technology is faster than SLA and allows for the creation of 3D objects with a lower volume of resin (De Leon et al. 2016). Additionally, DLP has the advantage of movable projector heads, which reduces build times by another 40 %. (Schweiger 2021). Despite these distinct advantages, DLP suffers from several limitations in terms of accuracy. Firstly, effects from the distribution of light and chemicals can cause material outside the desired pixel boundary to be cured, resulting in overcuring, and impairing the achievable resolution. Additionally, since each pixel has a square shape, printing features with rounded or angled shapes will produce a stair-step effect. The combination of these effects can lead to unwanted imperfections in the geometry (Montgomery et al. 2023).

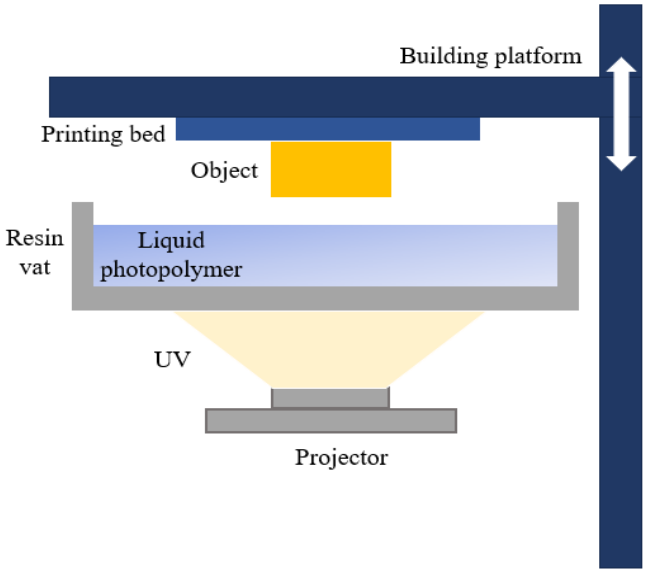

Figure 2. Schematic diagram of digital light processing technology.

2.3. FDM technology

The FDM technology is utilized in photopolymerization to melt a solid filament material in a nozzle, polymerize it as it is extruded, and stack it layer by layer (Kim 2022) (**Figure 3**).

The main advantages are that it is easy to handle in the clinic and can be used with most biomaterials. Furthermore, it is affordable and cost-effective. However, FDM is not widely adopted in dentistry due to its long printing time (Schweiger 2021), low dimensional accuracy, and susceptibility to thermal degradation, resulting in a rough surface (Daule 2013). High surface roughness, in particular, has been a major drawback that leads to low mechanical properties.

The common materials used in FDM are PLA (Polylactic Acid), ABS (Acrylonitrile Butadiene Styrene), PC (Polycarbonate), and PC-ABS blends (Polycarbonate-Acrylonitrile Butadiene Styrene). PLA and ABS resins are the most frequently used polymeric dental biomaterials for FDM technology. Due to the non-toxic properties of PLA in the oral cavity, it is considered more favorable for use in 3D printing compared to ABS (Barazanchi 2017, Turner 2014).

However, PLA has significant weaknesses and low impact resistance (Subramaniyan et al. 2022). To address these shortcomings, PLA parts are often combined with bio-carbon at various percentage levels of 5 %, 15 %, and 30 % to improve bonding (Ertane et al. 2018).

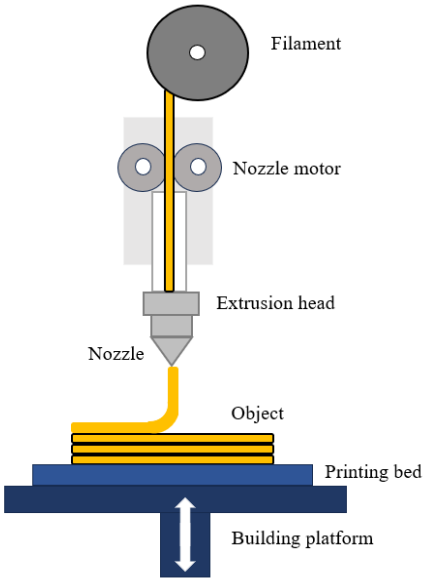

Figure 3. Schematic diagram of fused deposition modeling technology.

3. Importance of mechanical properties of temporary restoration

Temporary restoration supports natural teeth and periodontal tissues, protecting the pulpal tissue from bacterial contamination, physio-mechanical, and thermal irritation (Cha et al. 2020a). Depending on the patient's oral condition, temporary restoration is often a multi-step process and requires long-term maintenance, regardless of the duration (Ozel et al. 2017).

If a temporary crown has low mechanical properties, it may lead to a loss of vertical occlusion with the opposing teeth and changes in facial features due to the function of the masticatory system (Aldahian et al. 2021). As patients are keeping their natural teeth for many more years, the potential for mechanical properties becomes greater (Mair et al. 1996).

Therefore, temporary restorations must have sufficient physical and mechanical properties such as hardness, strength, impact resistance, and wear resistance, as these factors may affect the lifespan of the prosthesis (Abdullah 2018).

4. Selection of antagonists for wear resistance testing

The wear occurring between temporary restorations and the prosthesis is an important factor to consider during the extended temporary stage when making a final restoration decision in clinical practice.

Recently, zirconia and metal alloy have become popular in dentistry because of their superior mechanical properties. Several in vitro studies have evaluated the wear behavior of zirconia and metal alloys against different conventional milling materials. However, the wear behavior of zirconia and metal restorative materials is not well known when they oppose 3D-printed temporary resin crowns. It is meaningful to experiment with the wear pattern of the 3D printing temporary resin materials.

Thus, wear resistance should be implemented among the 3D-printed temporary resin crowns tested with zirconia and metal antagonists.

5. Influence of acidic environments

As mentioned earlier, temporary restoration often requires a long-term time. In other words, temporary restoration is naturally exposed to aging factors in the humid environment for a long time (Firlej et al. 2021), especially influences in saliva and food, pH environment as well as oral temperature (Szczesio-Wlodarczyk et al. 2020).

From a chemical perspective, temporary restoration is exposed to the structure of the polymer network by an aqueous environment (Ferracane 2006). Water particles fill the empty space between micro-gaps (Firlej et al. 2021). Then, water particles absorb into the resin matrix, causing swelling of the polymer resin matrix and making it more flexible (Drummond et al. 2009). The leaching of components, as well as degradation of the crosslinked matrix and hydrolysis in the interphase area, eventually lead to a decrease in mechanical properties (Takeshige et al. 2007) over time. Especially during daily life, changes in temporary restorations can promote bacterial growth due to a decrease in oral pH caused sugary food and drinks. Furthermore, this decrease in oral pH can also lead to an increase in plaque growth.

Previous studies have shown that the acidic fluids accelerate degradation through hydrolysis of the polymer matrix (Cilli 2012). The hydrolysis of the crystalline mainly works through a surface erosion mechanism (Farah 2016). The principle is that acidic fluids easily

penetrate the resin's polymer network, reducing its internal barrier force and resulting in increased flexibility (Drummond et al. 2009) and weakened mechanical properties (Rahim et al. 2012).

6. Research objectives

Recently, the digital industry has established itself as a major technology in the field of dentistry. Temporary dental restorations are also produced using various additive manufacturing technologies. However, existing studies of the physical properties and mechanical properties of temporary crown resin materials made using conventional and milled temporary crown resins have been reported. However, no comparison with 3D-printed temporary crown resins has been reported. Also, during daily life, changes in temporary restorations occur due to bacteria growth, as oral pH environments can be reduced by consuming sugary food and drinks. Furthermore, these oral low pH environments can induce plaque growth, thereby weakening mechanical properties. However, the influence of acidic pH on mechanical properties of temporary restorations fabricated by different additive manufacturing technologies has not yet been sufficiently studied.

Thus, the objective of this study was to investigate the influence of mechanical properties on temporary restorations produced from additive manufacturing technology when exposed to different acidic pH, as well as the mechanical properties of fabricated temporary resin specimens through different additive manufacturing technologies.

The null hypothesis was that there will be 1) no influence on the mechanical properties of temporary restorations produced from additive

manufacturing technology when exposed to different acidic pH, and 2) no differences in the mechanical properties of temporary resin specimens fabricated from different additive manufacturing technologies.

In addition, physical properties are significantly related to the water sorption parameter, so this study also implemented water absorption and solubility test.

II. MATERIALS AND METHODS

1. Preparations of temporary restoratives specimens produced from different additive manufacturing technology

This study design shows in **Figure 4.**

Each of the 180 rectangular parallelepipeds specimens (15 mm × 10 mm × 10 mm) (**Figure 5**), 60 bar shaped specimens (25 mm × 2 mm × 2 mm) (**Figure 6**), and 15 disk-shaped specimens (Ø15 mm × 1 mm) (**Figure 7**) were designed with Meshmixer (Autodesk Inc, California, USA), saved in STL files and exported to the 3D printing slicer software program (3D Sprint; 3D Systems).

Additive manufacturing was carried out with a SLA printer (Form2, Formlabs, Somerville, MA, USA) and High temp V2 resin (Vertex, Reutlingen, Germany), DLP printer (Asiga UV Max, Asiga, Alexandria, Australia) and Tera Harz TC-80DP (A2) (Graphy Inc., Seoul, Korea) as well as a FDM printer (CUBICON Single Plus – 320C, CUBICON Co. Ltd., Seoul, Korea) and Nexway PLA QA2-4 (QUVE Co. Ltd., Seoul, Korea). The chemical composition of the polymers used according to the manufacturers data are shown in **Table 1**.

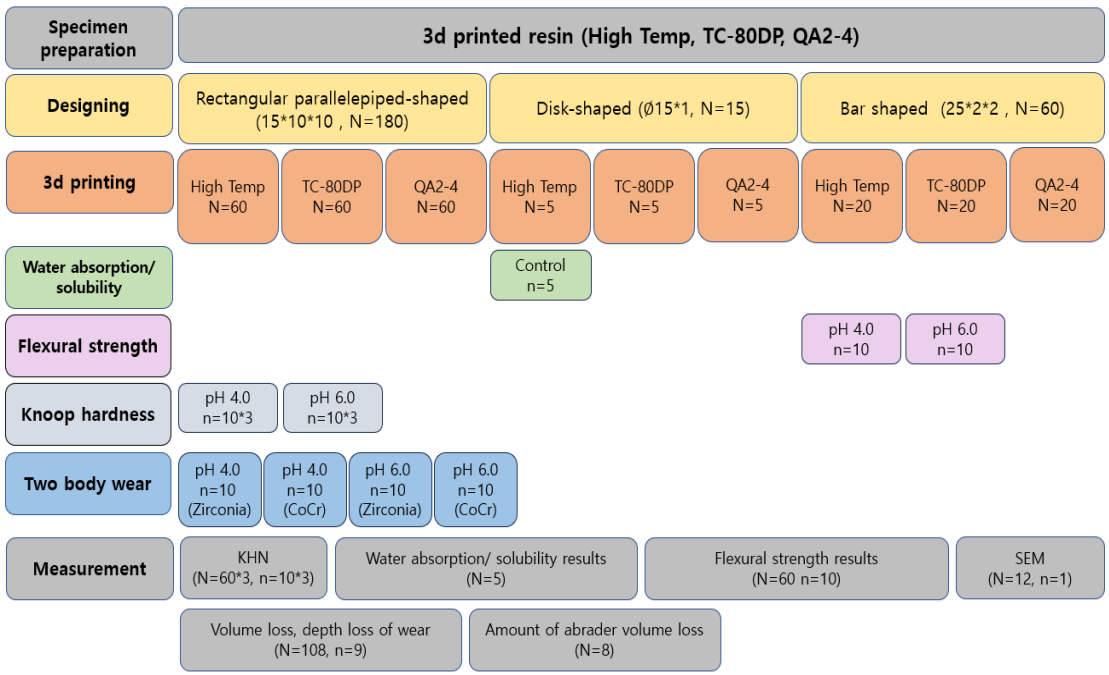

Figure 4. Study design flows diagram.

Table 1. Chemical composition of resin materials in this study

Resin Product	Resin Manufacturer	Composition	3D Printer	3D Printer Manufacturer
High-temp V2 resin	Formlabs, Inc., Somerville, MA, USA	Urethane dimthacrylate(UDMA) (25-45%) Acrylated monomer (40-60%) Photoinitiator (<1.5%)	Formlabs 2	Formlabs, Inc, Somerville, MA, USA
Tera Harz TC-80DP(A2)	Graphy Inc., Seoul, Korea	Urethane dimethacrylate-based resin phosphine oxides, pigment	Asiga UV Max	Asiga, Alexandria, Australia
Nexway QA2-4	QUVE Co. Ltd., Seoul, Korea	PLA (Poly lactic acid)	Single Plus-320	CUBICON Co. Ltd., Seoul, Korea

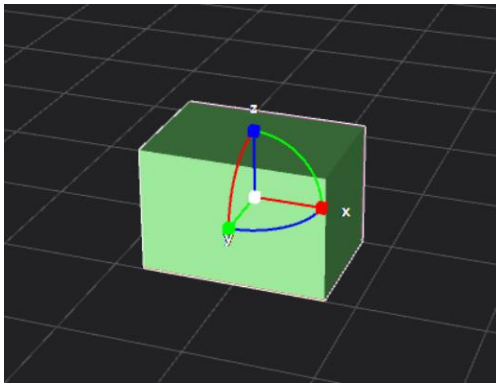

Figure 5. Rectangular parallelepipeds-shaped specimens (15 mm × 10 mm × 10 mm) design.

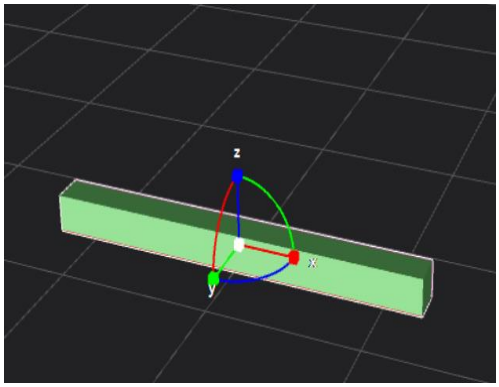

Figure 6. Bar-shaped specimens (25 mm × 2 mm × 2 mm) design.

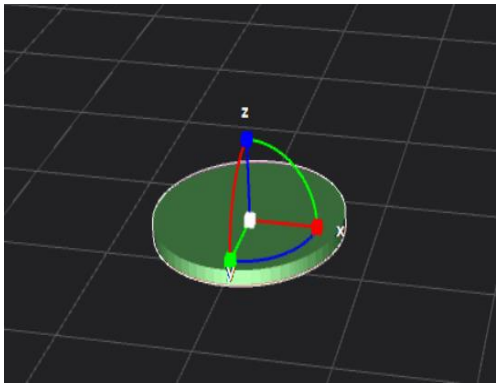

Figure 7. Disk-shaped specimens (Ø15 mm × 1 mm) design.

2. 3D-printed specimen fabrication

Cha et al., reported that the accuracy of the printed specimens showed the highest values at a 0° orientation, and the error was significantly low (Cha et al. 2020b). In addition, Tahayeri et al., reported that peak stress was higher in prints with a layer thickness of 100 μm (Tahayeri et al. 2018).

Thus, SLA and DLP specimens were printed with a build orientation of 0°, where the side to be tested was parallel to the build platform. The z-axis layer thickness set to 100 μm. The FDM specimens were printed with a build orientation of 0° orientation and a z-axis layer thickness of 200 μm. To achieve the ultimate strength, Rankouhi et al., recommends a layer thickness of 200 μm and a 0° orientation for FDM samples (Rankouhi et al. 2016).

2.1. SLA specimens

SLA is a method in which a light source emitted through a dotted laser point draws an output area and builds up. The specimens were printed with a build angle of 0° orientation and a z-axis layer thickness of 100 μm. After the 3D printing process (Form2, Formlabs, Somerville, MA, USA), the block was detached from the platform and washed for 5 minutes with 100 % isopropyl alcohol to remove excess resin monomers.

In the final stage, the specimens' post-curing temperature was set at 80 °C and for 120 min using a post-curing machine (Form cure printer, Formlabs, Somerville, MA, USA).

2.2. DLP specimens

In the case of DLP samples, the laser was controlled by a digital micro mirror and the entire layer of liquid resin was polymerized at once. Similarly, the specimens were printed with a build angle of 0 ° orientation and a z-axis layer thickness of 100 um. After the 3D printing process (Asiga UV Max, Asiga, Alexandria, Australia), the block detached from the platform and washed with 100 % isopropyl alcohol to remove excess resin monomers. In the final stage, the specimen was cured for 15 minutes using a nitrogen chamber (Tera Harz Cure, Graphy Inc., Seoul, Korea).

2.3. FDM specimens

For FDM samples, the file was transferred to Cubicreator program and printed using an FDM machine (CUBICON Single Plus – 320C, CUBICON Co. Ltd., Seoul, Korea). The specimens were printed with a build angle of 0°orientation. The printing layer thickness was fixed at 200 μm using a 0.4 mm nozzle. The extrusion temperature set at 200 °C, and the print speed was fixed at 60 mm/s. The temperature of the plate was set at 60 °C to ensure sufficient spreading of the first layer, facilitating a proper bond with the upper layers, as recommended by the manufacturer.

Afterwards, all samples were polished with silicon carbide paper of grain sizes 220 to 2000 grit on a rotary machine (Ecomet30, Bueheler Ltd, Lake Bluff, IL, USA) with water cooling.

3. Abrader specimen fabrication

The abrader, which was mounted on a chewing simulator to apply abrasive force to the specimens, was made of Zirconia and CoCr alloy. It was designed using software (Meshmixer, Autodesk Inc, California, USA) to have a hemisphere with a radius of 1.5 mm connected to a 10 mm cube via a 5 mm long neck (**Figure 8**). The design was based on the mesio-palatal cusp of the upper molar, the design of which has been used previously (Cha et al. 2020a).

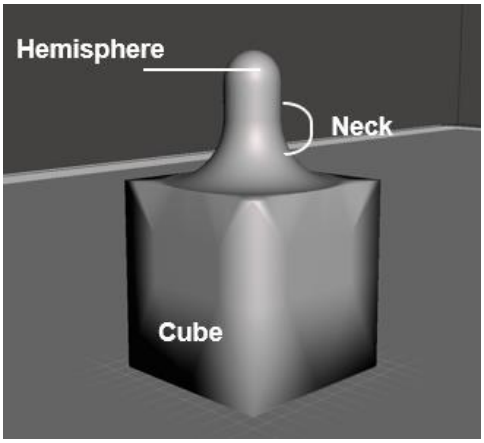

Figure 8. Abrader specimens design.

3.1. Zirconia abrader

The zirconia abrader was fabricated using a dry milling 5-axis milling machine (Arum5x-300 Hoil Dental, England, UK) from a disc-shaped tetragonal zirconia polycrystal-based block (ZirPremium UT+; Acucera Inc., Pochon, Korea). The sintering patterns were sintered according to the manufacturer's instructions. A fast-heating sintering process was utilized. This required the zirconia patterns be fired at 10 °C /minute up to 1000 °C (1,832 °F). After reaching 1000 °C, the patterns were fired at a rate of 3-5 °C /minute until a temperature of 1,500 °C was reached. The patterns were then held at this temperature for 2 hours and subsequently allowed to cool to room temperature prior to removal.

3.2. CoCr abrader

The metal abraders were made by a DMLS machine (EOSINT M270, EOS GmbH, Krailling, Germany) using CoCr powder (EOS Cobalt Chrome SP2, EOS GmbH, Krailling, Germany; Co: 62 - 66 wt-% Cr: 24 - 26 wt-% Mo: 5 –7 wt-%, Vikers hardness 420 HV). Its composition corresponds to type IV CoCr dental material in the EN ISO 22674:2006 standard.

In the DMLS machine, a steel base plate is mounted on the building platform. The top surface of the base plate is made parallel with respect to the recoating blade. A layer of iron powder is spread onto the steel base plate, which is then exposed to a laser beam to achieve sintering of powder. The build layer thickness was 20 um and a Yb-fibre laser point of 200 W was used (Ekren 2018).

The surface of the samples was then polished with a 1200 grit brown rubber point (Brownie Polisher PC2, SHOFU, Kyoto, Japan), while the polishing of the zirconia abrader surface was performed using a polishing kit (Soft Diamonds Grinding and Buffing Wheels; Asami Tanaka Dental, Friedrichsdorf, Germany). The abraders were polished with the full series of polishing discs rotating at approximately 10,000 rpm in a slow-speed handpiece (Ghazal 2008).

4. Exposure of temporary restorative specimens to artificial saliva with different acidity

The composition of the artificial saliva (AS) was prepared as follows : 0.4 g NaCl (Sigma-Aldrich, Steinheim, Germany), 0.4 g KCL (Duksan Pure Chemicals Co., Ansan-city, Korea), 0.795 g $CaCl_2$ (Sigma-Aldrich, Steinheim, Germany), 0.780 g $NaH_2PO_4 \cdot 2H_2O$ (Sigma-Aldrich, Steinheim, Germany), 0.005 g $Na_2S \cdot 9H2O$ (Junsei Chemical Co., Tokyo, Japan), and 1 g CH_4N_2O(Sigma-Aldrich, Steinheim, Germany) in 1L of solution (**Table 2**). Then, it was stirred for 24 h.

The solution was adjusted to pH 6.0 using 1.0 M NaOH (Duksan Pure Chemicals Co., Ansan-city, Korea) and pH 4.0 using 1.0 M HCl (Duksan Pure Chemicals Co., Ansan-city, Korea) (Kim et al. 2021). The pH levels were adjusted using a commercial pH meter (ORION™ Star A211, Thermo Scientific, Waltham, MA, USA).

The control group consisted of samples immersed in solutions with a pH of 6.0. The other half of the samples were immersed in acidic solutions with a pH of 4.0 and aged for one month under conditions simulating those of the oral environment at 37.

Table 2. Compositions of artificial saliva (AS)

Chemical formula	Content
NaCl	0.4 g
KCL	0.4 g
$CaCl_2$	0.795 g
$NaH_2PO_4 \cdot 2H_2O$	0.780 g
$Na_2S \cdot 9H_2O$	0.005 g
CH_4N_2O	1 g
NaOH	-
HCl	-
H_2O	1L

5. Water sorption and solubility

A total of 15 disk-shaped specimens (15 mm diameter × 1 mm thickness) were prepared in accordance with ISO 4049 (Standarization 2009).

First, the silica gel was placed on the bottom of the container and polished specimens were placed on top. The specimens were kept in a desiccator maintained at 37 ± 2 °C for 22 hours. Then, twenty-two hours later, samples were transferred into another desiccator at 23 ± 1 for 2 hours and weighed with an analytical balance (XS105, Mettler-toledo AG, Greifensee, Switzerland) with a ± 0.1 mg accuracy. This process was repeated when the mass of the specimen did not change by more than 0.1 mg, at which point the final weight was recorded as (*m1*). After drying each sample, two diameters perpendicular to each other were measured by an electronic digital caliper (Mitutoyo Model CD-15CPX, Mitutoyo Corporation, Kawasaki, Japan) with 0.01 mm accuracy and their mean was calculated. The thickness of the samples was measured at its center and at four spaced points at equal intervals along its circumference. The average diameter and thickness were used to calculate the volume (V). Each sample was separately immersed into 10 mL of distilled water in a water bath at 37 ± 1 for 7 days. Subsequently the surface water was dried about in the air for 15 seconds and weighed (*m2*) within 1 minute of its removal from the water. To calculate water sorption and solubility values,

the dehydration procedure was repeated until the samples acquired a constant mass, which was recorded as (*m3*).

The water sorption and solubility (μg/mm^3) of each material were calculated using formulas (1) and (2) as follows:

$$(1)\ \text{Water sorption} = \frac{m2-m3}{V}$$

$$(2)\ \text{Water solubility} = \frac{m1-m3}{V}$$

6. Knoop hardness test

A total of 60 rectangular parallelepiped-shaped specimens (15 m m length × 10 mm width × 10 mm height) were measured three times. To determine the Knoop hardness number (*KHN*), the speci mens were positioned centrally beneath the Knoop diamond indent er. The Knoop hardness tester (DMH-2, Matsuzawa Co. Ltd, Akit a, Japan) was used with a 500gf load and 15 seconds dwell time. The *KHN* was observed at a magnification of 100×. The *KHN* of each material was calculated using formula (3) as follows:

$$(3)\ KHN = 14.2 \times \frac{F}{d^2}$$

where F is the test load (gf) and d corresponds to the longer diagonal of an indentation in millimeters (Revilla-León et al. 2021).

7. Flexural strength test

A total of 60 bar-shaped specimens (25 mm length × 2 mm width × 2 mm height) were prepared. According to ISO 4049 (Standarization 2009), each specimen was positioned on a universal testing machine (Zwick Z010; Zwick, Ulm, Germany) equipped with a three-point bending jig, with a 20 mm length span between supports. The test was performed with a 50 N load under a crosshead speed of 1.0 mm/min until fracture. The maximum pressure before the breaking point was measured. Fracture loads were recorded using a commercial software program (testXpert II V3.3; Zwick, Ulm, Germany).

After the relevant data were collected, the flexural strength (*FS*) was calculated according to the following formula (4):

$$(4)\quad FS = \frac{3Fl}{2BH^2}$$

where F is the maximum load (N), L is the distance between supports (20 mm), B is the width of the specimen (mm), and H is the height of the specimen (mm).

8. Testing wear resistance using a chewing simulator

8.1. Wear test

A total of 120 rectangular parallelepiped-shaped specimens (15 m m length × 10 mm width × 10 mm height) were prepared.

Two body wear tests were performed using a chewing simulator (TW-T1000; Taewon TECH, Bucheon, Korea). Each specimen was mounted in the lower specimen metal jig, and the abraders were placed in the upper metal jig. Then, they were loaded with eight antagonist pairs simultaneously. The chewing cycle of the abrader was set to have 5 mm vertical descending movement, 2 mm horizontal movement (**Figure 9**).

Each specimen was abraded for 20,000 cycles, which is equivalent to one month of chewing from a clinical perspective, and a load of 5 kg, equivalent to the masticating force of 49 N each (Krejci et al. 1993). In addition, the specimens were subjected to thermocycling conditions of 5–55 ℃ by a heat/cool system for 60 seconds dwell time (**Table 3**).

At the end of one cycle, each specimen was air-dried and steam-cleaned to remove any dirt before scanning.

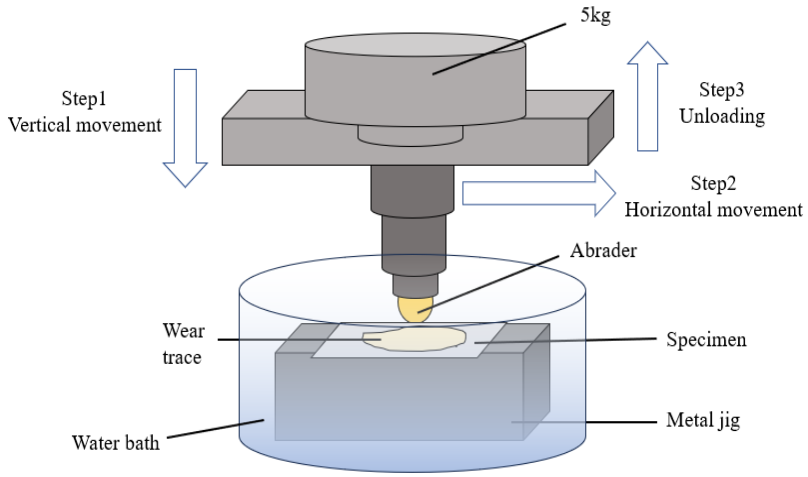

Figure 9. Schematic diagram of chewing simulation.

Table 3. Parameters of chewing simulator programmable logic

Parameter	Characteristics
Weight per samples	5 kg
Cycle frequency	1.2 Hz
Vertical movement	5 mm
Horizontal movement	2 mm
Cold/hot bath temperature	5 ℃/55 ℃
Dwell time	60 seconds

8.2. Scan

Following the chewing simulations, the Medit T710 (Medit T710, Seoul, South Korea) was used to measure accuracy of 4 μm (IOS12836) with Easy Scan Spray (Alphadent, Gyeonggi-Do, Korea). It utilizes blue-light scanning technology and incorporates a four 5.0 MP camera system (Falih, Majeed 2022). Afterward, the scan images were transferred to a USB memory card.

8.3. Quantitative volume loss and maximal depth of wear of specimens

The acquired images were imported into the GOM inspect mesh inspection software (GOM GmbH, Braunschweig, Germany). Then, the GOM Volume Inspect Pro mesh inspection software (GOM GmbH, Braunschweig, Germany) was aligned with specimens before and after the chewing simulations to quantify the maximal depth loss and volume loss of wear. To analyze surface wear, all specimens were cut 2 mm below the worn part.

The amount of volume loss (mm^3) by chewing simulation was calculated by subtracting the volume of the specimens after the chewing simulations from the volume before the chewing simulations. The amount of depth loss (mm) was calculated by subtracting the total height of the specimens after the chewing simulations from the total height before the chewing simulations.

8.4. Qualitative assessment of wear using Field-Emission Scanning Electron Microscopy (FE-SEM)

The qualitative wear analysis was performed by visualizing specimens using field emission scanning electron microscopy. A thin platinum coating was applied to the worn surface using a sputter coater (Quorum Q150T-S, Quorum Technologies, West Sussex, UK), and the specimens were observed with a field emission scanning electron microscope (FE-SEM) (Hitachi S-4700, Hitachi High-Technologies Group, Schaumburg, IL, USA) at 50 x magnifications at the end of the wear tests.

8.5. Quantitative volume loss of abrader

For the quantification of wear on the abrader, the acquired images were imported into the GOM inspect mesh inspection software (GOM GmbH, Braunschweig, Germany). Subsequently, the quantification of volume loss due to wear was measured using the GOM Volume Inspect Pro mesh inspection software (GOM GmbH, Braunschweig, Germany) aligned with the abrader before and after the chewing simulations. Then, the abrader was cut 2 mm down from the worn part. The amount of volume loss (mm^3) from the chewing simulations was calculated using the method described earlier with the resin specimens (**Figure 10**).

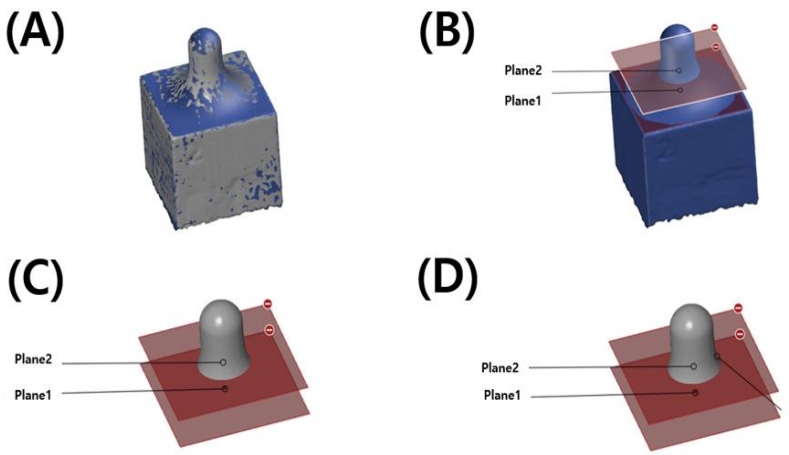

Figure 10. Abrader's wear measurement steps; (A) aligning abraders before and after chewing simulation, (B) cutting 2 mm down from the worn part, (C) cut-out abraders and (D) calculating volume loss by subtracting the abrader's volume, respectively, after the chewing simulations from that of the abraders before the chewing simulations.

9. Statistical analysis

Statistical analysis was performed using SPSS Statistics 26 software (IBM, Armonk, NY, USA). One-way ANOVA and Tukey's post-hoc analysis were performed for water solubility and absorption, Knoop hardness, flexural strength, and wear resistance. The Mann-Whitney test was performed for the abrader groups in the wear resistance tests. A t-test was performed to determine influence of acidic pH. The statistical significance level for all tests was set at a p-value < 0.05.

III. RESULTS

1. Water sorption/ solubility

Water sorption and solubility were found to have statistically significant differences among 3D-printed resin groups ($p < 0.05$) (**Table 4**).

The average value of water sorption was highest for the DLP group 23.16 ± 1.33^{a}, followed by the SLA group 21.16 ± 2.19^{ab}, and FDM group 18.33 ± 2.68^{b} ($p < 0.05$).

The average value of water solubility was highest for the FDM group 0.003 ± 0.0030^{a}, followed by the SLA group -0.011 ± 0.0030^{b}, and the DLP group -0.015 ± 0.0021^{b} ($p < 0.05$).

Table 4. Water sorption and solubility data are expressed as mean ± standard deviation for the specimens

Group	Wsp (μg/mm^3)	Wsl (μg/mm^3)
SLA	21.16 ± 2.19^{ab}	-0.011 ± 0.0030^{b}
DLP	23.16 ± 1.33^{a}	-0.015 ± 0.0021^{b}
FDM	18.33 ± 2.68^{b}	0.003 ± 0.0030^{a}

The same lowercase letters indicate no statistically significant difference between results in accordance with additive manufacturing (AM) methods ($p > 0.05$).

2. Knoop hardness test

The Knoop hardness values (*KHN*) of the 3D-printed specimens are presented in **Table 5** and **Figure 11**.

The mean ± standard deviations values for Knoop hardness in the presence of pH 4.0 were 22.64 ± 1.98 for the SLA group, 22.15 ± 1.18 for the DLP group, and 15.26 ± 1.81 for the FDM group. For pH 6.0, the results were 24.96 ± 0.87 for the SLA group, 23.39 ± 0.94 for the DLP group, and 19.32 ± 0.82 for the FDM group.

There were no significant differences in Knoop hardness between the SLA and DLP groups at both pH levels ($p > 0.05$). However, the FDM group showed significant differences with both the SLA and DLP groups at both pH levels ($p < 0.05$).

In addition, all specimens immersed in artificial saliva with a pH of 4.0 resulted in significantly lower Knoop hardness values than specimens immersed in a pH of 6.0 ($p < 0.05$), regardless of additive manufacturing technology.

Table 5. Knoop hardness (*KHN*) expressed as mean ± standard deviation for specimens at various pH values

AM Methods	Knoop hardness (*KHN*) Mean ± Standard deviation	
	pH 4.0	pH 6.0
SLA	22.64 ± 1.98^{Ab}	24.96 ± 0.87^{Aa}
DLP	22.15 ± 1.18^{Ab}	23.39 ± 0.94^{Aa}
FDM	15.26 ± 1.81^{Bb}	19.32 ± 0.82^{Ba}

The same capital letters indicate no statistically significant difference between results in accordance with additive manufacturing (AM) methods ($p > 0.05$). The same lowercase letters indicate no statistically significant difference between specimens immersed in pH 4.0 and pH 6.0 ($p > 0.05$).

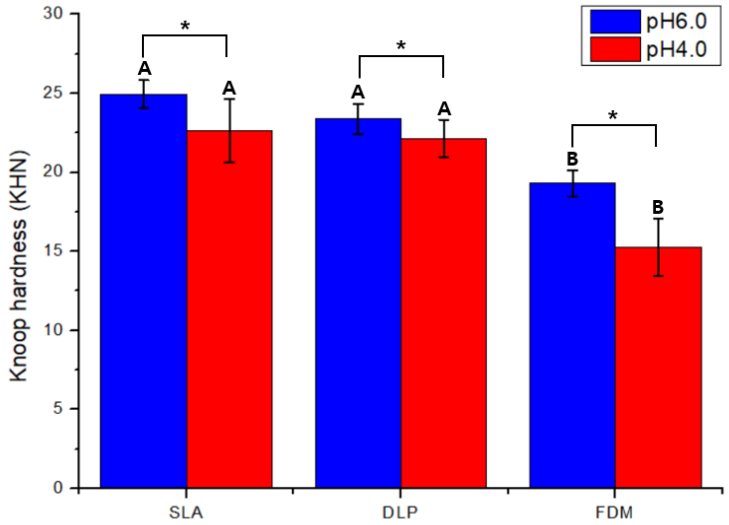

Figure 11. Knoop hardness (*KHN*) expressed as mean ± standard deviation for specimens at various pH values. '*' indicates a statistically significant difference between pH 6.0 and pH 4.0 ($p < 0.05$). The same capital letters indicate no statistically significant difference between results in accordance with additive manufacturing (AM) methods ($p > 0.05$).

3. Flexural strength test

The flexural strength (MPa) of the 3D-printed specimens is presented in **Table 6** and **Figure 12**.

The mean ± standard deviation values for flexural strength in the presence of pH 4.0 were (101.96 ± 4.49) MPa for the SLA group, (100.35 ± 4.32) MPa for the DLP group, and (80.30 ± 6.48) MPa for the FDM group. For pH 6.0, the results were (106.74 ± 3.99) MPa for the SLA group, (104.83 ± 3.32) MPa for the DLP group, and (82.73 ± 6.31) MPa for the FDM group.

There were no significant differences in flexural strength between the SLA and DLP group at both pH levels ($p > 0.05$). However, the FDM group showed significant differences with both the SLA and DLP group at both pH levels ($p < 0.05$).

In addition, all specimens immersed in artificial saliva with a pH of 4.0 resulted in significantly lower flexural strength than specimens immersed in a pH 6.0 ($p < 0.05$), regardless of the AM technology.

Table 6. Flexural strength expressed as mean ± standard deviation for specimens at various pH values

AM Methods	Flexural strength (MPa) Mean ± Standard deviation	
	pH 4.0	pH 6.0
SLA	101.96 ± 4.49^{Ab}	106.74 ± 3.99^{Aa}
DLP	100.35 ± 4.32^{Ab}	104.83 ± 3.32^{Aa}
FDM	80.30 ± 6.48^{Bb}	82.73 ± 6.31^{Ba}

The same capital letters indicate no statistically significant difference between results in accordance with additive manufacturing (AM) methods ($p > 0.05$). The same lowercase letters indicate no statistically significant difference between specimens immersed in pH 4.0 and pH 6.0 ($p > 0.05$).

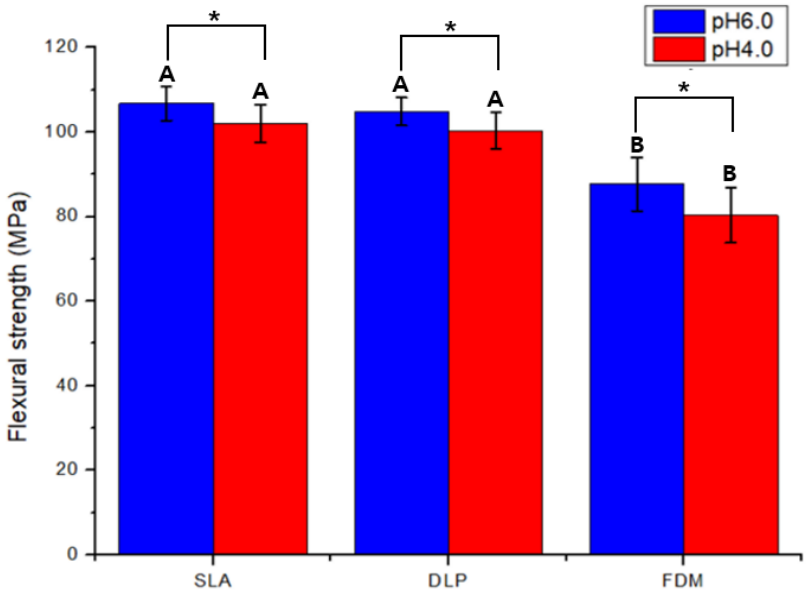

Figure 12. Flexural strength (MPa) expressed as mean ± standard deviation for specimens at various pH values. '*' indicates statistically significant difference between pH 6.0 and pH 4.0 ($p < 0.05$). The same capital letters indicate no statistically significant difference between results obtained using additive manufacturing (AM) methods ($p > 0.05$).

4. Surface wear Assessment

4.1. Quantitative results for wear loss of volume

The wear loss in volume of the 3D-printed specimens after the chewing simulations is presented in **Table 7** and **Figure 13**.

The mean ± standard deviation values for wear loss in volume against the zirconia abrader in the presence of pH 6.0 were (2.42 ± 0.42) mm^3 for the SLA group, (2.49 ± 0.47) mm^3 for the DLP group, and (4.06 ± 1.86) mm^3 for the FDM group. For pH 4.0, the results were (2.98 ± 0.55) mm^3 for the SLA group, (3.00 ± 0.23) mm^3 for the DLP group, and (5.74 ± 1.41) mm^3 for the FDM group.

There were no significant differences in the volume loss between the SLA and DLP group in both pH ($p > 0.05$). However, the FDM group showed significant differences with both the SLA and DLP groups in both pH conditions ($p < 0.05$).

Additionally, all specimens immersed in artificial saliva at pH 4.0 resulted in significantly more wear loss of volume than specimens immersed in pH 6.0 ($p < 0.05$), regardless of additive manufacturing technology used.

The mean ± standard deviations values for wear loss in volume against the metal abrader in the presence of pH 6.0 were (2.70 ± 0.54) mm^3 for the SLA group, (2.78 ± 0.44) mm^3 for the DLP group, and

(4.09 ± 0.99) mm^3 for the FDM group. In the presence of pH 4.0, the results were (3.30 ± 0.78) mm^3 for the SLA group, (3.67 ± 0.38) mm^3 for the DLP group, and (6.78 ± 0.94) mm^3 for the FDM group.

Similar to the results when the zirconia abrader was used, there were no significant differences in the volume loss between the SLA and DLP groups ($p > 0.05$) in both pH conditions. However, the FDM group showed significant differences with both the SLA and DLP groups ($p < 0.05$) in both pH conditions.

Additionally, all specimens immersed in artificial saliva at pH 4.0 resulted in significantly more wear loss of volume than specimens immersed in pH 6.0 ($p < 0.05$), regardless of the additive manufacturing technology used.

Table 7. The wear loss of volume expressed as mean ± standard deviation for specimens at various pH values

AM Methods	Wear loss of volume (mm^3) Mean ± Standard deviation			
	Zirconia Abrader		Metal (CoCr) Abrader	
	pH 4.0	pH 6.0	pH 4.0	pH 6.0
SLA	2.98 ± 0.55^{Ba}	2.42 ± 0.42^{Bb}	3.30 ± 0.78^{Ba}	2.70 ± 0.54^{Bb}
DLP	3.00 ± 0.23^{Ba}	2.49 ± 0.47^{Bb}	3.67 ± 0.38^{Ba}	2.78 ± 0.44^{Bb}
FDM	5.74 ± 1.41^{Aa}	4.06 ± 1.86^{Ab}	6.78 ± 0.94^{Aa}	4.5 ± 0.99^{Ab}

The same capital letters indicate no statistically significant difference between results in accordance with additive manufacturing (AM) methods ($p > 0.05$). The same lowercase letters indicate no statistically significant difference between specimens immersed in pH 4.0 and pH 6.0 ($p > 0.05$).

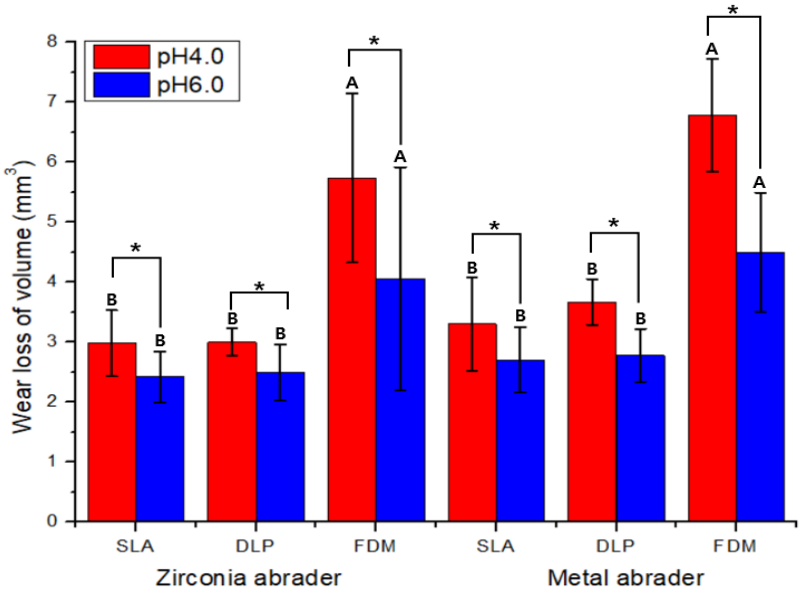

Figure 13. Wear a loss of volume (mm^3) expressed as mean ± standard deviation for specimens at various pH values, with different abrader (zirconia and metal). '*' indicates statically significant difference between pH 6.0 and pH 4.0 ($p < 0.05$). The same capital letters indicate no statistically significant difference between results in accordance with additive manufacturing (AM) methods ($p > 0.05$).

4.2. Quantitative results for wear loss of maximal depth

The wear loss of the maximal depth of the 3D-printed specimens after the chewing simulations is presented in **Table 8** and **Figure 14**.

The mean wear loss of the maximal depth ± standard deviations against the zirconia abrader in the presence of pH 6.0 was (0.18 ± 0.04) mm for the SLA group, (0.21 ± 0.03) mm for the DLP group, and (1.21 ± 0.22) mm for the FDM group. In the presence of pH 4.0, the results were (0.22 ± 0.03) mm for the SLA group, (0.26 ± 0.06) mm for the DLP group, and (2.31 ± 0.58) mm for the FDM group.

There were no significant differences in the wear loss of the maximal depth between the SLA and DLP groups for both pH ($p > 0.05$). However, the FDM group showed significant differences with both the SLA and DLP groups for both pH ($p < 0.05$).

In addition, all specimens immersed in artificial saliva of pH 4.0 resulted in significantly more wear loss of maximal depth than specimens immersed in pH 6.0 ($p < 0.05$), regardless of AM technology.

The mean wear loss of the maximal depth ± standard deviations against the metal abrader in the presence of pH 6.0 was (0.21 ± 0.04) mm for the SLA group, (0.25 ± 0.04) mm for the DLP group, and (1.38 ± 0.37) mm for the FDM group. In the presence of pH 4.0, the results were (0.27 ± 0.02) mm for the SLA group, (0.33 ± 0.08) mm for the DLP group, and (2.65 ± 0.27) mm for the FDM group.

There were no significant differences in the wear loss of the maximal depth between the SLA and DLP groups in both pH ($p > 0.05$). However, the FDM group showed significant differences with both the SLA and DLP groups, in both pH ($p < 0.05$).

In addition, all specimens immersed in artificial saliva of pH 4.0 resulted in significantly more wear loss of the maximal depth than specimens immersed in pH 6.0 ($p < 0.05$), regardless of AM technology.

Table 8. The wear loss of maximal depth expressed as mean ± standard deviation for specimens at various pH values

AM Methods	Wear loss of maximal depth (mm) Mean ± Standard deviation			
	Zirconia Abrader		Metal (CoCr) Abrader	
	pH 4.0	pH 6.0	pH 4.0	pH 6.0
SLA	0.22 ± 0.03^{Ba}	0.18 ± 0.04^{Bb}	0.27 ± 0.02^{Ba}	0.21 ± 0.04^{Bb}
DLP	0.26 ± 0.06^{Ba}	0.21 ± 0.03^{Bb}	0.33 ± 0.08^{Ba}	0.25 ± 0.04^{Bb}
FDM	2.31 ± 0.58^{Aa}	1.21 ± 0.22^{Ab}	2.65 ± 0.27^{Aa}	1.38 ± 0.37^{Ab}

The same capital letters indicate no statistically significant difference between results in accordance with additive manufacturing (AM) methods ($p > 0.05$). The same lower-case letters indicate no statistically significant difference between specimens immersed in pH 4.0 and pH 6.0 ($p > 0.05$)

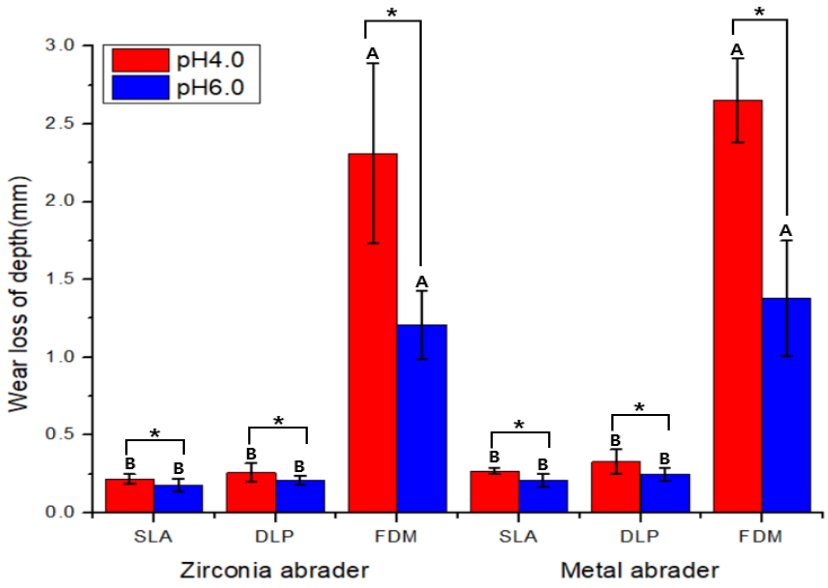

Figure 14. Wear a loss of maximal depth (mm) expressed as mean ± standard deviation for specimens at various pH values, with different abrader (zirconia and metal). '*' indicates statistically significant difference between pH 6.0 and pH 4.0 ($p < 0.05$). The same capital letters indicate no statistically significant difference between results in accordance with additive manufacturing (AM) methods ($p > 0.05$).

4.3. Qualitative results of wear on the printed specimens

The FE-SEM images of the worn surfaces of the specimens after the wear tests are shown in (**Figure 15 and 16**). All types of resin showed cracks and dented features.

For the SLA resin specimens, a smooth surface with small cracks and grooves oriented parallel with the sliding direction were observed (**Figure 15** and **16** (A1-A4)). The DLP resin specimens showed slightly wider range of grooves and dented fractures (**Figure 15** and **16 (**B1-B4)). For the FDM resin specimens, remarkably more wide range of cracks and sharp step of the layer were observed (**Figure 15** and **16 (**C1-C4)).

In the presence of pH 6.0 specimens, a smooth surface with small steps on the fractured surface was seen for the specimen (**Figure 15** (A1, B1, C1), **Figure 16** (A3, B3, C3)), while pH 4.0 specimens remarkably distributed wrinkles-like appearance and patchy surface were observed (**Figure 15** (A2, B2, C2), **Figure16** (A4, B4, C4)).

Additionally, the surfaces of the wear areas of the three materials in contact with the zirconia abrader appeared to be relatively smoother than those in contact with the CoCr alloy abrader (**Figure 15**). For the CoCr alloy abrader, the features relatively showed a rough surface with faint lamellae (**Figure 16**). All resin specimens changed from a smooth to rough surface with layering fracture.

Based on FE-SEM findings there were variations in surface in term of

different AM technologies type and different pH solutions influence, especially the appearance of surface layering fracture with acidic pH solutions and when used to CoCr alloy abrader ($p > 0.05$).

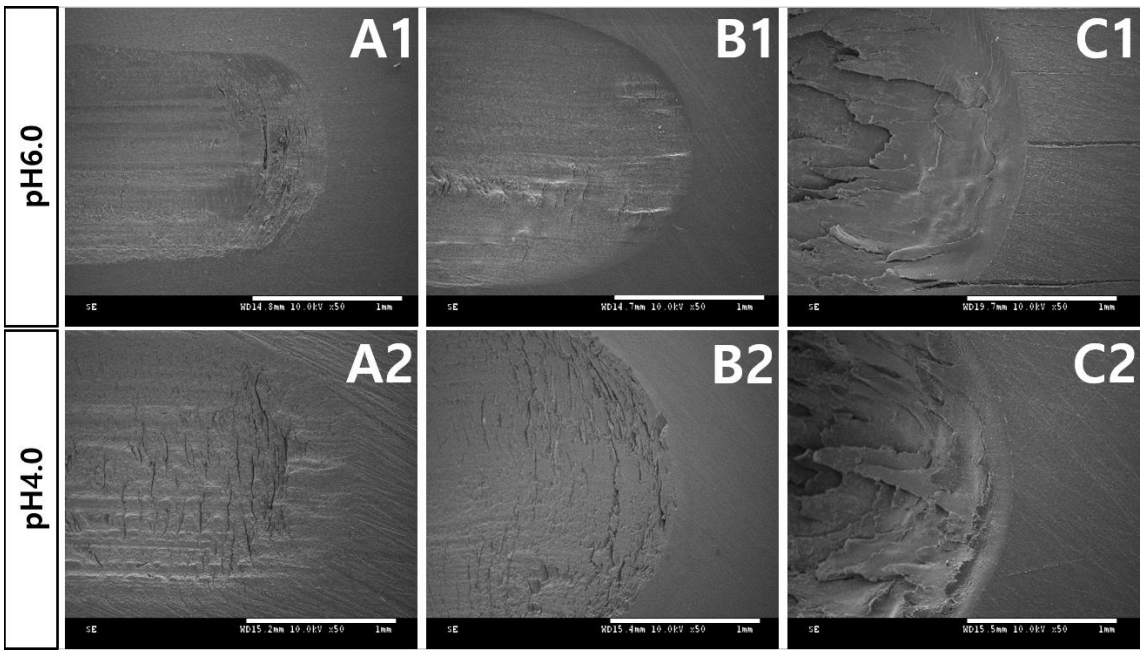

Figure 15. FE-SEM images of the worn surfaces of the materials against the zirconia abrader. SLA specimens (A1-A2); DLP specimens (B1–B2); FDM specimens(C1–C2); under different pH solutions (4.0, and 6.0). The scale bar is 1 mm.

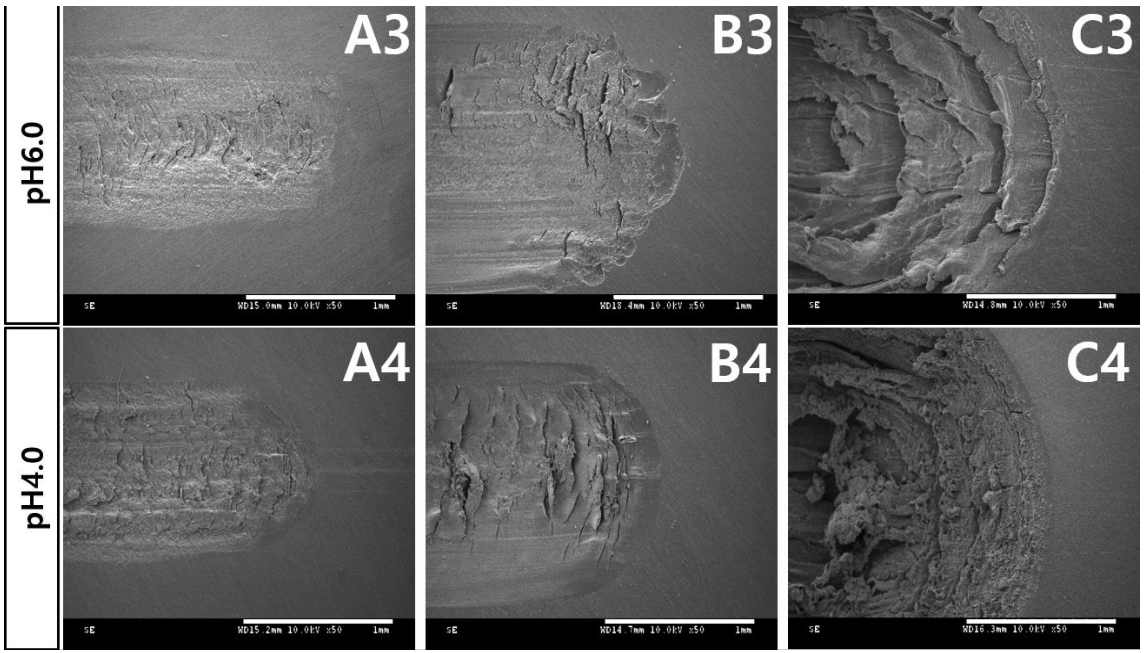

Figure 16. FE-SEM images of the worn surfaces of the materials against the metal abrader. SLA specimens (A3-A4); DLP specimens (B3–B4); FDM specimens(C3–C4); under different pH solutions (4.0, and 6.0). The scale bar is 1 mm.

4.4. Quantitative results of abrader wear loss of volume

In this study, zirconia and metal abrader were used to simulate wear. Two-body wear tests, loaded with eight antagonist pairs simultaneously, were carried out, allowing each abrader's measurement to influence 300,000 cycles. **Table 9** indicates that there was no significant difference in volume loss between the abraders ($p > 0.05$), but when looking at the specimens, volume loss and depth loss deviation were generally lower when zirconia was instead of CoCr alloy as the abrader.

In scanning electron microscopy images, the surfaces of the wear areas of the three materials in contact with the zirconia abrader appeared to be relatively smoother than those in contact with the CoCr alloy abrader.

Table 9. Wear loss of volume is expressed as mean ± standard deviation for the abrader

	Abrader wear loss of volume (mm^3) **Mean ± Standard deviation**
Zirconia abrader	0.17 ± 0.02[a]
Metal (CoCr) abrader	0.19 ± 0.02[a]

The same lowercase letters indicate no statistically significant difference between abraders ($p > 0.05$).

IV. DISCUSSION

This results of this study demonstrated (1) an influence in acidic pH and (2) a difference in mechanical properties among temporary resin specimens fabricated from different AM technologies, and, therefore, the null hypothesis was rejected.

1. Influence of acidic pH environments

It is important that the mechanical properties influence in acidic pH environments.

The effects of acidity are more destructive in the case of internal stress in the material structure. Previous studies have shown that acidity accelerates degradation due to hydrolysis of the polymer matrix (Cilli 2012). Hydrolysis of the crystalline mainly works through surface erosion mechanism (Farah 2016). Thus, when immersed acidic fluids, they easily penetrate the polymer network of resin and reduce the internal barrier force, resulting in more flexibility (Drummond et al. 2009) and weak mechanical properties (Rahim et al. 2012).

In this study, the mechanical properties were measured by varying the concentration of the pH solutions. In a previous *in vitro* study, a pH of 4.0 was usually used as the lowest pH in plaque (Prakki et al. 2005), and salivary pH generally ranges between 6 and 7 (Alshahrani et al. 2022).

Thus, this present study sets up pH 4.0 and pH 6.0. All specimens tested in this study showed that acidic solutions of pH 4.0 decrease surface hardness, flexural strength, and wear resistance, which is in agreement with previous studies (Alzaid et al. 2022, Chadwick et al. 1990, Firlej et al. 2021, Yilmaz et al. 2018). Influence of acidic environments also definitively showed worn surface after two body wear tests in the SEM images.

In the presence of pH 6.0 specimens, a smooth surface with small steps on the fractured surface was seen for the specimens (**Figure 15** (A1, B1, C1), **Figure 16** (A3, B3, C3)). However, pH 4.0 specimens remarkably displayed a wrinkled-like appearance and patchy surface (**Figure 15** (A2, B2, C2), **Figure 16** (A4, B4, C4)).

Especially, the results showed that the FDM group had significantly lower values after immersion in the acidic solution of pH 4.0. The reason for this can be attributed to the quick diffusion of the acidic solution of pH 4.0 from the interior of the high-porosity devices (Farah 2016). The PLA component printed by FDM has inferior moisture barrier characteristics compared with synthetic polymers (Pan et al. 2008), and it is easily hydrolyzed by moisture (Yew et al. 2005).

Thus, management of the moisture environment and hydrolytic degradation of PLA are significantly sensitive factors.

2. Physical properties

Water sorption and solubility

The mechanical properties related to water sorption and solubility.

In this study, the SLA and DLP groups showed no significant differences compared to the FDM group ($p > 0.05$). The water sorption values of the DLP group were 23.16 ± 1.33^{a}, followed by the SLA group values of 21.16 ± 2.19^{ab}. Additionally, the water solubility of the DLP group were -0.015 ± 0.021^{b}, while the SLA group values were -0.011 ± 0.0030^{b}.

The SLA and DLP groups are commonly used in UDMA resin matrix. As a result, higher water sorption follows, however, negative water solubility values for the UDMA resin matrix. This resin matrix seems to be related to the hydrophilicity characteristic (Szczesio-Wlodarczyk et al. 2021). When resins are absorbed in water, unreacted monomers and small oligomers are eluted, and water is trapped in the space between the polymer chains (Szczesio-Wlodarczyk et al. 2021). UDMA resin matrix primarily consists of polar groups of the resin molecules, so it can be concluded that these materials absorb water molecules that are not released. After these resin materials are bonded by water molecules chemically (Tuna et al. 2008).

Contrastively, the FDM group exhibited relatively low water sorption 18.33 ± 2.68[b] and high-water solubility 0.003 ± 0.0030[a]. These results can be attributed to the hydrophobic characteristic of the PLA content (Choi et al. 2023).

Based on the water sorption and solubility results, it is expected that the FDM group would demonstrate good mechanical properties. However, the mechanical properties of the tested FDM group exhibited remarkably poor results.

This is likely due to the high-porosity nature of the PLA component printed by FDM, resulting in poor toughness, lower impact resistance (Subramaniyan et al. 2022). Additionally, the material was found to be very brittle. As a result, its usage is limited to certain applications (Farah 2016).

3. Mechanical properties

3.1. Knoop hardness test

In this study, the surface hardness test was determined according to the Knoop method.

There were no significant differences in the surface hardness between the tested SLA and DLP groups ($p > 0.05$). However, the FDM group showed significant differences with both the SLA and DLP groups ($p < 0.05$). The reason for the superior mechanical properties of the SLA and DLP groups compared to the FDM group is explained by the photocrosslinkable materials used in photopolymerization. These materials consist of intermolecular interactions, which influence the better chemical, mechanical properties and modulus of crosslinked dimethacrylate systems (Gajewski et al. 2012). Moreover, UDMA component printed by the SLA and DLP groups had a flexible nature, lower viscosity of 23 Pa·s, and lower MW = 470 g/mol (Sideridou 2002).

In addition, UDMA is relatively composed of small- sized molecules (Kessler et al. 2019), resulting in a higher concentration of double bonds (Barszczewska-Rybarek 2020) and the formation of a tight network (Sideridou 2002). Due to the correlation between the degree of conversion and hardness (Ferracane 1985), the UDMA component printed by the SLA and DLP groups demonstrated positive results.

3.2. Flexural strength test

The flexural strength was evaluated based on a three-point bending test according to ISO 4049. The ISO 4049 demands a flexural strength of at least 80 MPa for restorative materials (ISO 2009). The temporary restorations obtained in this study will allow the requirements of the standard.

There were no significant differences in the flexural strength between the tested SLA and DLP groups ($p > 0.05$). However, the FDM group showed significant differences with both the SLA and DLP groups ($p < 0.05$).

From a chemical perspective, high values were demonstrated in the tested properties of UDMA components. UDMA components have been characterized by greater stiffness and resistance to three-point bending (Szczesio-Wlodarczyk et al. 2021), resulting in positive effects.

3.3. Surface wear assessment

The wear resistance was evaluated based on two body wear tests.

One of the most influential manufacturing factors affecting wear performance is build orientation. Previous study results suggest that specimens printed at 90° were more prone to fracture (KEßLER 2021, Park et al. 2019). In addition, printed specimens demonstrate that as the printing orientation decreases, the mechanical properties increases (Lee et al. 2022, Lužanin 2014). Thus, all 3D-printed specimen were fabricated at 0° of build orientation in this study. However, another previous study demonstrated a different influence of build orientation on the wear test.

Mohamed et al., found that specimen fabricated at 0° of build orientation have long sliding molecular chains, which leads to high frictional heating and higher temperature, eventually resulting in molecular reorientation and chain scission (Mohamed et al. 2017) (**Figure 17**).

In contrast, specimens fabricated at 90° of build orientation generate shorter raster lengths that are parallel to the sliding surface. The molecular cannot move as much between layers, and thus it leads to a drop in the wear rate (Mohamed et al. 2017).

Dangnan et al., also demonstrated a lower wear rate when the test specimens are orientated perpendicular to the sliding direction compared

to the parallel orientation (Dangnan et al. 2020).

The present study found that the amount of the SLA group was similar to that of the DLP group ($p > 0.05$). The volume loss and maximal depth loss of wear also showed similar patterns. However, the worn surface of the DLP group exhibited a slightly wider range of grooves and dented features in the SEM images (**Figure 15 (**B1, B2), **Figure 16** (B3, B4)).

In contrast, the FDM group showed significant differences compared to both the SLA and DLP groups ($p < 0.05$). The maximal depth loss and volume loss values were remarkably large. SEM images revealed a wider range of cracks and sharp steps between layers (**Figure 15** (C1, C2), **Figure 16** (C3, C4)). Thus, the impact of FDM printing on the fatigue mechanism was analyzed. Shanmugam et al., demonstrated that FDM printing has the ability to produce polymer materials compared to conventional methods. However, the formation of porosity and imperfections in FDM printed polymers is an inevitable characteristic that can result in failure under loading (Shanmugam et al. 2021). Additionally, FDM printed materials are anisotropic due to the lack of uniform strength in all directions, resulting from layer-to-layer adhesion and interlayer voids. The primary process parameters of FDM include layer thickness, infill pattern, infill density, air gap, and build orientation (Tanveer et al. 2022). Higher infill density (100 %) during manufacturing improves interlayers bonding and provides more

resistance to deformation due to a reduced air gap (**Figure 18**) (Camargo et al. 2019). Furthermore, Tanveer et al., reported that increasing infill percentage enhances the mechanical properties (Tanveer et al. 2022). The layer thickness affects the filament strength (Gomez-Gras et al. 2018).

As the layer thickness increases, mechanical properties improve (Camargo et al. 2019). To achieve ultimate strength, Rankouhi et al., recommend using 0.2 mm layer thickness and 0° orientation samples (Rankouhi et al. 2016). The infill pattern controls the build time, amount of filament, and strength of the FDM parameter, making it an important factor. Camargo et al., revealed that mechanical properties improve as the linear infill pattern parameter increases (Camargo et al. 2019). For this reason, FDM specimens fabricated according to the above reference in this study. Differences in wear patterns were found between the materials depending on the abraders. There was no significant difference in volume loss between the abraders ($p > 0.05$), but when examining the specimens, volume loss and depth loss deviation were generally lower when zirconia was used compared to when the CoCr alloy was used as the abraders.

Additionally, the surfaces of the wear areas of the specimens in contact with the zirconia abrader appeared relatively smooth in the SEM images. The differences in the results may be attributed to the presence or absence

of fillers and the nature of the fillers (Cha et al. 2020b). Also the CoCr alloy used in the DMLS method during the solidification of melting metal, in particular “Co”, can enhance crack tendency (Béreš et al. 2018).

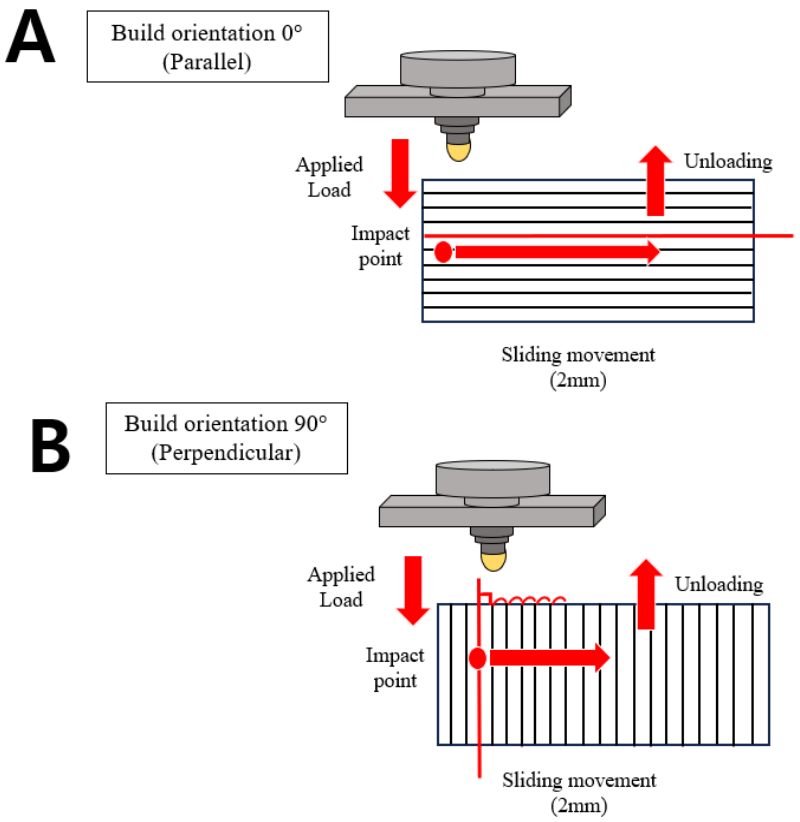

Figure 17. Effects of build orientation in two body wear tests.

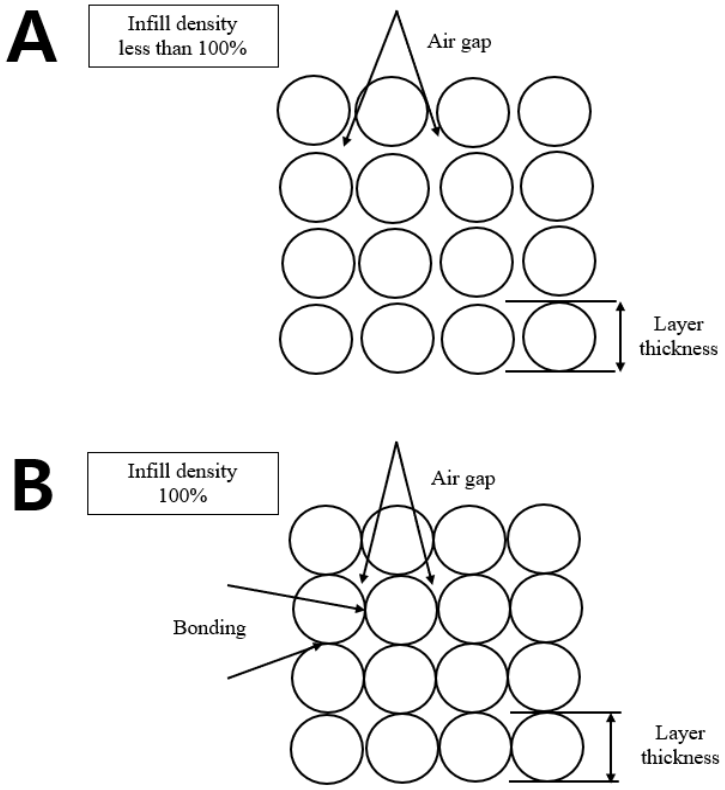

Figure 18. Difference according to amount of Infill density and air gap.

The two body wear test parameters were as similar as possible to the clinical loading conditions. The load of 5 kg was equivalent to the average masticatory force of 49 N each. In addition, force ranges of 0.4 to 0.75 N and cycles ranging from 10,000 to 1,200,000 were adopted for most wear tests. A cycle of 250,000 loadings is similar to about one year in clinical situations (DeLong et al. 1985). Thus, 20,000 cycles of load are comparable to approximately one year of chewing from a clinical perspective. However, depending on the condition of the patient, the temporary restorations may consist of multiple units of prosthesis, and the period of use may be extended depending on periodontal or implant surgery.

This study had a limitation in that it is an *in vitro* study.

First, these specimens had a flat surface, whereas teeth and restorations have complicated shapes that cause different stresses at various sites on the restoration surface (Mair et al. 1996). Second, several *in vitro* wear studies have demonstrated the wear performance of dental restorations that encourage the reproduction of the *in vivo* masticatory system (Lambrechts et al. 2006). However, it is not practically possible to precisely simulate the masticatory movements in oral environments using *in vitro* simulators (Altaie 2017, Lee 1975).

Third, wear resistance tests such as three body wear tests may be even more clinically important compared to two body wear tests

(McCabe et al. 2002). While three-body wear may yield meaningful results for predicting clinical performance, they are likely to offer limited assistance in assessing material characteristics.

In this study, the surface hardness, flexural strength, and wear resistance of three different types of 3D-printed resin were evaluated, and the results showed that the SLA and DLP specimens could yield stable clinical outcomes compared to those of the FDM specimens.

Using an FDM printer to produce temporary restorations is relatively less available compared to other 3D printers. However, according to existing literature, internal fit and mechanical properties within clinically acceptable ranges (Kim 2022). Although there is still insufficient evidence regarding the utility of temporary restorations made with PLA, ongoing research aims to enhance mechanical strength by incorporating additives such as bio-carbon and carbon black, ensuring consistent output and high quality. In the future, temporary restorations printed with FDM printer can be produced highly versatile.

Dietary habits expose temporary restorations to factors such as sugary food and acidic drinks. According to existing studies, temporary restorations can be subject to the polymer network structure in a pH environment.

Consequently, water particles fill the empty spaces between micro-gaps (Firlej et al. 2021). The results, including leaching of the

components, degradation of the crosslinked matrix, and hydrolysis in the interphase area, eventually lead to a decrease in mechanical properties over time (Takeshige et al. 2007).

Thus, this study investigates the influence of acidic pH on the mechanical properties of temporary restorations fabricated using various additive manufacturing technologies. The results reveal that under acidic conditions with a pH of 4.0, poor mechanical properties were observed.

Consequently, managing acidity in the oral environment emerges as a significantly sensitive that must be carefully considered.

V. CONCLUSION

While some comparative studies on the mechanical properties of materials produced using conventional milling methods have been reported, there is no comparison with the 3D printing method in the existing literature.

Furthermore, the influence of acidic pH on the mechanical properties of temporary restorations, fabricated using various additive manufacturing technologies, has not been sufficiently studied.

Thus, the aim of this study was to investigate the influence of acidic pH and mechanical properties of fabricated temporary resin specimens through different AM technologies. With the limitation that this was an in vitro experiment, the results showed that the SLA and DLP groups could yield stable clinical outcomes compared to those of the FDM group.

Additionally, under acidic conditions, poor mechanical properties were observed. Thus, considerable attention is required for acidity in the oral environment.

VI. REFERENCES

Abdullah. "Comparison between direct chairside and digitally fabricated temporary crowns." *Dental materials journal* 37, no. 6 (2018): 957-63.

Aldahian, Nada, Khan, Rawaiz, Mustafa, Mohammed, Vohra, Fahim, Alrahlah, Ali. "Influence of Conventional, CAD-CAM, and 3D Printing Fabrication Techniques on the Marginal Integrity and Surface Roughness and Wear of Interim Crowns." *Applied sciences (Basel, Switzerland)* 11, no. 19 (2021): 8964.

Alshahrani, Faris A, AlToraibily, Fatemah, Alzaid, Maryam, Mahrous, Amr A, Al Ghamdi, Maram A, Gad, Mohammed M. "An Updated Review of Salivary pH Effects on Polymethyl Methacrylate (PMMA)-Based Removable Dental Prostheses." *Polymers* 14, no. 16 (2022): 3387.

Altaie. "An approach to understanding tribological behaviour of dental composites through volumetric wear loss and wear mechanism determination; beyond material ranking." *Journal of Dentistry* 59 (2017): 41-7.

Alzaid, Maryam, AlToraibily, Fatemah, Al-Qarni, Faisal D, Al-Thobity, Ahmad M, Akhtar, Sultan, Ali, Saqib, Al-Harbi, Fahad A, Gad, Mohammed M. "The effect of salivary pH on the flexural strength and surface properties of CAD/CAM denture base materials." *European Journal of Dentistry* 17, no. 01 (2022): 234-41.

Barazanchi. "Additive technology: update on current materials and applications in dentistry." *Journal of Prosthodontics* 26, no. 2 (2017): 156-63. doi:https://doi.org/10.1111/jopr.12510.

Barszczewska-Rybarek. "Novel urethane-dimethacrylate monomers and compositions for use as matrices in dental restorative materials." *International journal of molecular sciences* 21, no. 7 (2020): 2644.

Béreš, M, Silva, CC, Sarvezuk, PWC, Wu, L, Antunes, LHM, Jardini, AL, Feitosa, ALM, Žilková, J, de Abreu, HFG. "Mechanical and phase

transformation behaviour of biomedical Co-Cr-Mo alloy fabricated by direct metal laser sintering." *Materials Science and Engineering: A* 714 (2018): 36-42.

Camargo, José C, Machado, Álisson R, Almeida, Erica C, Silva, Erickson Fabiano Moura Sousa. "Mechanical properties of PLA-graphene filament for FDM 3D printing." *The International Journal of Advanced Manufacturing Technology* 103 (2019): 2423-43.

Cha, H. S., Park, J. M., Kim, T. H., Lee, J. H. "Wear resistance of 3D-printed denture tooth resin opposing zirconia and metal antagonists." *J Prosthet Dent* 124, no. 3 (2020a): 387-94. doi:10.1016/j.prosdent.2019.09.004.

Cha, Hyun-Suk, Park, Ji-Man, Kim, Tae-Hyung, Lee, Joo-Hee. "Wear resistance of 3D-printed denture tooth resin opposing zirconia and metal antagonists." *The Journal of Prosthetic Dentistry* 124, no. 3 (2020b): 387-94. doi:https://doi.org/10.1016/j.prosdent.2019.09.004.

Chadwick, RG, McCabe, JF, Walls, AWG, Storer, R. "The effect of storage media upon the surface microhardness and abrasion resistance of three composites." *Dental Materials* 6, no. 2 (1990): 123-8.

Choi, Won-Il, Yoo, Lee-gang, Kim, Yu-ri, Jung, Bock-Young. "Mechanical properties of CAD/CAM polylactic acid as a material for interim restoration." *Heliyon* 9, no. 4 (2023).

Cilli. "Properties of dental resins submitted to pH catalysed hydrolysis." *Journal of dentistry* 40, no. 12 (2012): 1144-50.

Dangnan, F, Espejo, C, Liskiewicz, T, Gester, M, Neville, A. "Friction and wear of additive manufactured polymers in dry contact." *Journal of Manufacturing Processes* 59 (2020): 238-47.

Daule, VM. "Rapid prototyping and its application in dentistry." *Journal of Dental & Allied Sciences* 2, no. 2 (2013): 57-61.

DeLong, Ralph, Sakaguchi, RL, Douglas, William H, Pintado, MR. "The wear

of dental amalgam in an artificial mouth: a clinical correlation." *Dental Materials* 1, no. 6 (1985): 238-42. doi:https://doi.org/10.1016/S0109-5641(85)80050-6.

Drummond, James L, Lin, Lihong, Al-Turki, Lulwa A, Hurley, Ryan K. "Fatigue behaviour of dental composite materials." *Journal of Dentistry* 37, no. 5 (2009): 321-30.

Ekren. "Effect of layered manufacturing techniques, alloy powders, and layer thickness on metal-ceramic bond strength." *The Journal of Prosthetic Dentistry* 119, no. 3 (2018): 481-7.

Ertane, Ertan G, Dorner-Reisel, Annett, Baran, Ozlem, Welzel, Thomas, Matner, Viola, Svoboda, Stefan. "Processing and wear behaviour of 3D printed PLA reinforced with biogenic carbon." *Advances in Tribology* 2018 (2018).

Falih, Mina Yahia, Majeed, Manhal A. "Trueness and Precision of Eight Intraoral Scanners with Different Finishing Line Designs: A Comparative In Vitro Study." *European Journal of Dentistry* (2022).

Farah. "Physical and mechanical properties of PLA, and their functions in widespread applications—A comprehensive review." *Advanced drug delivery reviews* 107 (2016): 367-92.

Ferracane, Jack L. "Correlation between hardness and degree of conversion during the setting reaction of unfilled dental restorative resins." *Dental Materials* 1, no. 1 (1985): 11-4.

———. "Hygroscopic and hydrolytic effects in dental polymer networks." *Dental Materials* 22, no. 3 (2006): 211-22.

Firlej, Marcel, Pieniak, Daniel, Niewczas, Agata M, Walczak, Agata, Domagała, Ivo, Borucka, Anna, Przystupa, Krzysztof, Igielska-Kalwat, Joanna, Jarosz, Wojciech, Biedziak, Barbara. "Effect of artificial aging on mechanical and tribological properties of CAD/CAM composite materials used in dentistry." *Materials* 14, no. 16 (2021): 4678.

Gajewski, Vinícius ES, Pfeifer, Carmem S, Fróes-Salgado, Nívea RG, Boaro, Letícia CC, Braga, Roberto R. "Monomers used in resin composites: degree of conversion, mechanical properties and water sorption/solubility." *Brazilian dental journal* 23 (2012): 508-14.

Ghazal. "Wear resistance of nanofilled composite resin and feldspathic ceramic artificial teeth." *The Journal of Prosthetic Dentistry* 100, no. 6 (2008): 441-8.

Gomez-Gras, Giovanni, Jerez-Mesa, Ramón, Travieso-Rodriguez, J Antonio, Lluma-Fuentes, Jordi. "Fatigue performance of fused filament fabrication PLA specimens." *Materials & Design* 140 (2018): 278-85.

ISO. "Dentistry—Polymer-based restorative materials." *Geneve: International Organization for Standardization* (2009).

Javaid. "Current status and applications of additive manufacturing in dentistry: A literature-based review." *Journal of oral biology and craniofacial research* 9, no. 3 (2019): 179-85. doi:https://doi.org/10.1016/j.jobcr.2019.04.004.

KEßLER. "In vitro investigation of the influence of printing direction on the flexural strength, flexural modulus and fractographic analysis of 3D-printed temporary materials." *Dental Materials Journal* 40, no. 3 (2021): 641-9.

Kessler, Andreas, Reymus, Marcel, Hickel, Reinhard, Kunzelmann, Karl-Heinz. "Three-body wear of 3D printed temporary materials." *Dental Materials* 35, no. 12 (2019): 1805-12.

Kim, Eun-Kyong. "Three-dimensional printing of temporary crowns with polylactic acid polymer using the fused deposition modeling technique: a case series." *Journal of Yeungnam Medical Science* (2022).

Kim, M., Lee, M., Kim, K., Yang, S., Seo, J., Choi, S., Kwon, J. "Enamel Demineralization Resistance and Remineralization by Various Fluoride-Releasing Dental Restorative Materials." *Materials* 14, no. 16 (2021).

Krejci, Ivo, Lutz, F, Reimer, M, Heinzmann, JL. "Wear of ceramic inlays, their

enamel antagonists, and luting cements." *The Journal of Prosthetic Dentistry* 69, no. 4 (1993): 425-30. doi:https://doi.org/10.1016/0022-3913(93)90192-Q.

Lambrechts, Paul, Debels, Elke, Van Landuyt, Kirsten, Peumans, Marleen, Van Meerbeek, Bart. "How to simulate wear?: overview of existing methods." *Dental materials* 22, no. 8 (2006): 693-701.

Lee. "Surface roughness of composite filling materials." *Biomaterials, Medical Devices, and Artificial Organs* 3, no. 4 (1975): 503-19.

Lee, Hakjun, Son, Keunbada, Lee, Du-Hyeong, Kim, So-Yeun, Lee, Kyu-Bok. "Comparison of Wear of Interim Crowns in Accordance with the Build Angle of Digital Light Processing 3D Printing: A Preliminary In Vivo Study." *Bioengineering* 9, no. 9 (2022): 417.

Lee, Sangho. "Prospect for 3D Printing Technology in Medical, Dental, and Pediatric Dental Field." *J Korean Acad Pediatr Dent* 43, no. 1 (2016): 93-108. doi:10.5933/JKAPD.2016.43.1.93.

Ligon, Samuel Clark, Liska, Robert, Stampfl, Jürgen, Gurr, Matthias, Mülhaupt, Rolf. "Polymers for 3D printing and customized additive manufacturing." *Chemical reviews* 117, no. 15 (2017): 10212-90.

Lužanin. "Effect of layer thickness, deposition angle, and infill on maximum flexural force in FDM-built specimens." *Journal for Technology of Plasticity* 39, no. 1 (2014): 49-58.

Mair, LH, Stolarski, TA, Vowles, RW, Lloyd, CH. "Wear: mechanisms, manifestations and measurement. Report of a workshop." *Journal of dentistry* 24, no. 1-2 (1996): 141-8. doi:https://doi.org/10.1016/0300-5712(95)00043-7.

McCabe, JF, Molyvda, S, Rolland, SL, Rusby, S, Carrick, TE. "Two-and three-body wear of dental restorative materials." *International Dental Journal* 52 (2002): 406-16.

Mohamed, Omar Ahmed, Masood, Syed Hasan, Bhowmik, Jahar Lal, Somers,

Anthony E. "Investigation on the tribological behavior and wear mechanism of parts processed by fused deposition additive manufacturing process." *Journal of Manufacturing Processes* 29 (2017): 149-59.

Montgomery, S Macrae, Demoly, Frédéric, Zhou, Kun, Qi, H Jerry. "Pixel-Level Grayscale Manipulation to Improve Accuracy in Digital Light Processing 3D Printing." *Advanced Functional Materials* (2023): 2213252.

Mukhtarkhanov, Muslim. "Application of stereolithography based 3D printing technology in investment casting." *Micromachines* 11, no. 10 (2020): 946.

Ozel, Gulsum Sayin, Guneser, Mehmet Burak, Inan, Ozgur, Eldeniz, Ayce Unverdi. "Evaluation of C. Albicans and S. Mutans adherence on different provisional crown materials." *The Journal of Advanced Prosthodontics* 9, no. 5 (2017): 335-40.

Pan, Pengju, Liang, Zhichao, Zhu, Bo, Dong, Tungalag, Inoue, Yoshio. "Roles of physical aging on crystallization kinetics and induction period of poly (L-lactide)." *Macromolecules* 41, no. 21 (2008): 8011-9.

Pandey, Ramji. "Photopolymers in 3D printing applications." (2014).

Park, Sang-Mo, Park, Ji-Man, Kim, Seong-Kyun, Heo, Seong-Joo, Koak, Jai-Young. "Comparison of flexural strength of three-dimensional printed three-unit provisional fixed dental prostheses according to build directions." *Journal of Korean Dental Science* 12, no. 1 (2019): 13-9.

Prakki, Anuradha, Cilli, Renato, Mondelli, Rafael Francisco Lia, Kalachandra, Sid, Pereira, José Carlos. "Influence of pH environment on polymer based dental material properties." *Journal of dentistry* 33, no. 2 (2005): 91-8.

Rahim, Tuan Noraihan Azila Tuan, Mohamad, Dasmawati, Akil, Hazizan Md, Ab Rahman, Ismail. "Water sorption characteristics of restorative dental composites immersed in acidic drinks." *Dental Materials* 28, no. 6 (2012): e63-e70.

Rankouhi, Behzad, Javadpour, Sina, Delfanian, Fereidoon, Letcher, Todd. "Failure analysis and mechanical characterization of 3D printed ABS with respect to layer thickness and orientation." *Journal of Failure Analysis and Prevention* 16 (2016): 467-81.

Revilla-León, Marta, Morillo, Jorge Alberto, Att, Wael, Özcan, Mutlu. "Chemical composition, Knoop hardness, surface roughness, and adhesion aspects of additively manufactured dental interim materials." *Journal of Prosthodontics* 30, no. 8 (2021): 698-705.

Schweiger. "3D Printing in Digital Prosthetic Dentistry: An Overview of Recent Developments in Additive Manufacturing." *Journal of Clinical Medicine* 10, no. 9 (2021): 2010.

Shanmugam, Vigneshwaran, Das, Oisik, Babu, Karthik, Marimuthu, Uthayakumar, Veerasimman, Arumugaprabu, Johnson, Deepak Joel, Neisiany, Rasoul Esmaeely, Hedenqvist, Mikael S, Ramakrishna, Seeram, Berto, Filippo. "Fatigue behaviour of FDM-3D printed polymers, polymeric composites and architected cellular materials." *International Journal of Fatigue* 143 (2021): 106007.

Sideridou. "Effect of chemical structure on degree of conversion in light-cured dimethacrylate-based dental resins." *Biomaterials* 23, no. 8 (2002): 1819-29.

Soman, Pranav, Chung, Peter H, Zhang, A Ping, Chen, Shaochen. "Digital microfabrication of user-defined 3D microstructures in cell-laden hydrogels." *Biotechnology and bioengineering* 110, no. 11 (2013): 3038-47.

Standarization, International Organization for. "Dentistry—Polymer-Based Restorative Materials; ISO 4049-2009." (2009).

Subramaniyan, Madheswaran, Karuppan, Sivakumar, Radhakrishnan, K, Kumar, R Rajesh, Kumar, K Saravana. "Investigation of wear properties of 3D-printed PLA components using sandwich structure–A review." *Materials Today: Proceedings* (2022). doi:https://doi.org/10.1016/j.matpr.2022.04.913.

Szczesio-Wlodarczyk, Agata, Domarecka, Monika, Kopacz, Karolina, Sokolowski, Jerzy, Bociong, Kinga. "An evaluation of the properties of urethane dimethacrylate-based dental resins." *Materials* 14, no. 11 (2021): 2727.

Szczesio-Wlodarczyk, Agata, Sokolowski, Jerzy, Kleczewska, Joanna, Bociong, Kinga. "Ageing of dental composites based on methacrylate resins—A critical review of the causes and method of assessment." *Polymers* 12, no. 4 (2020): 882.

Tahayeri, Anthony, Morgan, MaryCatherine, Fugolin, Ana P, Bompolaki, Despoina, Athirasala, Avathamsa, Pfeifer, Carmem S, Ferracane, Jack L, Bertassoni, Luiz E. "3D printed versus conventionally cured provisional crown and bridge dental materials." *Dental materials* 34, no. 2 (2018): 192-200.

Takeshige, F, Kawakami, Y, Hayashi, M, Ebisu, S. "Fatigue behavior of resin composites in aqueous environments." *Dental Materials* 23, no. 7 (2007): 893-9.

Tanveer, Md Qamar, Mishra, Gautam, Mishra, Siddharth, Sharma, Rohan. "Effect of infill pattern and infill density on mechanical behaviour of FDM 3D printed Parts-a current review." *Materials Today: Proceedings* 62 (2022): 100-8.

Tian, Yueyi, Chen, ChunXu, Xu, Xiaotong, Wang, Jiayin, Hou, Xingyu, Li, Kelun, Lu, Xinyue, Shi, HaoYu, Lee, Eui-Seok, Jiang, Heng Bo. "A review of 3D printing in dentistry: Technologies, affecting factors, and applications." *Scanning* 2021 (2021).

Tuna, Suleyman Hakan, Keyf, Filiz, Gumus, Hasan Onder, Uzun, Cengiz. "The evaluation of water sorption/solubility on various acrylic resins." *European journal of dentistry* 2, no. 03 (2008): 191-7.

Turner. "A review of melt extrusion additive manufacturing processes: I. Process design and modeling." *Rapid prototyping journal* 20, no. 3 (2014): 192-204.

Unkovskiy. "Objects build orientation, positioning, and curing influence dimensional accuracy and flexural properties of stereolithographically printed

resin." *Dental Materials* 34, no. 12 (2018): e324-e33. doi:https://doi.org/10.1016/j.dental.2018.09.011.

Yew, GH, Yusof, AM Mohd, Ishak, ZA Mohd, Ishiaku, US. "Water absorption and enzymatic degradation of poly (lactic acid)/rice starch composites." *Polymer Degradation and stability* 90, no. 3 (2005): 488-500.

Yilmaz, Efe Çetn, Sadeler, Recep, Duymuş, Zeynep Yeşil, Özdoğan, Alper. "Effect of ambient pH and different chewing cycle of contact wear on dental composite material." *Dentistry and Medical Research* 6, no. 2 (2018): 46-50.

ABSTRACT (IN KOREAN)

다양한 산도에 따른 3D 프린팅 임시 크라운 레진 재료의 기계적 특성

<지도교수 권 재 성>

연세대학교 대학원 치의학과

최 명 지

3D 프린팅이라고도 불리는 적층 제조 기술이 발달하며 다양한 적층 제조 기술을 활용한 치과용 임시 수복물이 제작되고 있다. 또한, 단 음식 및 음료 섭취로 인하여 이러한 임시 수복물은 다양한 산성도(acidity)에 노출되게 된다.

이에 본 연구는 서로 다른 적층 제조 기술을 사용하여 제작된 치과용 임시 레진 크라운 시편의 기계적 특성뿐만 아니라 산성에 노출되었을 때의 기계적 특성을 연구하였다.

총 180 개의 직육면체 모양의 시편, 60 개의 바 모양의 시편 그리고 15 개의 디스크 모양의 시편을 Stereo Lithography Apparatus (SLA), Digital Light Processing (DLP) 및 Fused Deposition Modelling (FDM)의 세 가지 유형의 제조 방법으로 준비하였다. 모든 기계적 강도 시험은 두 가지의 산성도인 pH 4.0과 pH 6.0에서 진행되었다.

물리적 특성을 확인하기 위해 물 흡수도 용해도 시험을 평가하였다. 또한 기계적 특성을 확인하기 위해 표면 경도 시험, 굴곡 강도 시험, 마모저항성 시험을 평가하였다. 요구사항에 맞는 검증을 위하여 물 흡수도 용해도 시험과 굴곡강도 시험은 ISO 4049에 따라 평가하였다. 표면 경도 시험은 각 시편당 15 초 동안 500 g의 하중을 가하였고 3번씩 반복 측정하였다. 마모저항성 실험을 위해서는 3 종류의 시편과 지르코니아와 코발트 크롬합금의 대합치를 사용하였다. 마모도 시험 시 각 시편은 수직으로 5 mm, 수평으로 2 mm 움직이도록 설정되었고 이를 총 20,000 번 반복하였으며 5 kg 하중으로 저작 힘

을 가하도록 설정하였다. 비교를 위해 One-way ANOVA, Tukey's post-hoc analysis, Mann-Whitney, T-test를 사용하였다.

SLA와 DLP 그룹의 경우 적층 제조 기술에 따른 마모저항성 시험, 표면 경도 시험, 굴곡 강도 시험 결과에서 두 그룹 간의 유의미한 차이를 보이지 않았다 ($p > 0.05$). 하지만 FDM 그룹은 마모저항성 시험, 표면경도 시험, 굴곡강도 시험 결과에서 SLA와 DLP 두 그룹에 비해 유의차 있게 감소하였다 ($p < 0.05$).

산성도를 고려할 때에는 적층 제조 기술에 상관없이 마모저항성 실험 결과에서 모든 시편이 pH 4.0에 노출되었을 때 최대 깊이 및 마모 손실량이 pH 6.0 일 때 보다 유의차 있게 증가하였고($p < 0.05$), 표면경도, 굴곡강도 시험 결과에서는 모든 시편이 pH 4.0에 노출되었을 때 pH 6.0일 때 보다 유의차 있게 감소하였다($p < 0.05$). 본 연구 결과, 세 가지 유형의 적층 제조 기술로 제작된 임시 수복물 재료의 기계적 특성에서 SLA 및 DLP 레진 시편이 FDM 레진 시편에 비해 안정적인 임상 결과를 얻을 수 있는 것으로 나타났으며 pH가 낮은 산성도 환경에서 기계적 특성이 낮아지는 것을 확인하였다. 이에 임상적으로 적층 제조 기술을 활용하여 임시 수복물을 제작하

였을 때 어떠한 방식으로 적층 제조할지 결정과 산성도에 대한 주의가 필요할 것으로 사료된다.

핵심되는 말: 적층 제조 기술, SLA, DLP, FDM, 치과용 임시 수복물, 산성, 기계적 특성